THE DECARBONYLATION OF ALDEHYDES USING RUTHENIUM PORPHYRINS

by

BLAITHIN TARPEY

B.Sc., University College, Galway, 1977

A THESIS SUBMITTED IN PARTIAL FULFILMENT OF

THE REQUIREMENTS FOR THE DEGREE OF

MASTER OF SCIENCE

in

THE FACULTY OF GRADUATE STUDIES

(Chemistry)

We accept this thesis as conforming

to the required standard

THE UNIVERSITY OF BRITISH COLUMBIA

In presenting this thesis in partial fulfilment of the requirements for an advanced degree at the University of British Columbia, I agree that the Library shall make it freely available for reference and study. I further agree that permission for extensive copying of this thesis for scholarly purposes may be granted by the head of my department or by his or her representatives. It is understood that copying or publication of this thesis for financial gain shall not be allowed without my written permission.

Department of CHEMISTRY

The University of British Columbia
2075 Wesbrook Place
Vancouver, Canada
V6T 1W5

Date 29th March 1982.

ABSTRACT

The topic of this thesis is the catalytic and stoichiometric decarbonylation of aldehydes. A carbonylation reaction, the reaction of $RuTPP(n\text{-}Bu_3P)_2$ with CO gas was also studied.

A catalytic decarbonylation system, using $RuTPP(PPh_3)_2$ as catalyst plus added excess tri-n-butylphosphine in acetonitrile-dichloromethane, was employed to decarbonylate several organic aldehydes. This system proved to be an effective decarbonylation agent, which also exhibited some selectivity. Some mechanistic studies were carried out in an attempt to elucidate the details of the reaction mechanism. From these and other findings in this laboratory, a tentative mechanism was proposed for the decarbonylation reaction. A radical mechanism, involving Ru(III) intermediates was favoured on the basis of e.s.r. data, spectral evidence and cyclic voltammetry studies. However, no intermediates were isolated. The full details of the mechanism, such as the precise nature of the postulated intermediates, have not been fully determined, although there are indications that solvated species, like $RuTPP(CO)(CH_3CN)$, may be important. The stoichiometric reaction between $RuTPP(n\text{-}Bu_3P)_2$ and phenylacetaldehyde was also studied. The kinetic analysis indicated that the reaction, equation i,

$$RuTPP(n\text{-}Bu_3P)_2 + C_6H_5CH_2CHO \longrightarrow RuTPP(CO)(n\text{-}Bu_3P) + n\text{-}Bu_3P + C_6H_5CH_3$$

equation i

followed a pseudo-first-order rate law in the absence of excess phosphine, however, the actual k obsd values were found to be irreproducible. Some features of this reaction, such as the failure of the reaction to go to

completion, and also the effect of trace oxygen on the reaction were investigated.

The carbonylation of RuTPP(n-$Bu_3P)_2$ by CO gas was of interest, with respect to the catalytic reaction, which seems to involve pre-treatment with CO (or aldehyde) to form a phosphine monocarbonyl. The reaction was found to follow a simple dissociative mechanism, which is similar to that observed for analogous M(porp)L_2, where M = Ru or Fe. A K value of 0.054 at 26°C was obtained and individual rate constants were calculated also. The temperature dependence of K was used to find the thermodynamic parameters $\Delta S°$ and $\Delta H°$ for the reaction.

Some electrochemical studies were performed on RuTPP(n-$Bu_3P)_2$ and the corresponding monocarbonyl, RuTPP(CO)(n-Bu_3P). Electrochemical oxidation of RuTPP(CO)(n-Bu_3P) yielded a π-cation radical, whereas bromine oxidation appeared to effect oxidation of the metal.

TABLE OF CONTENTS

LIST OF TABLES

LIST OF FIGURES

Abbreviations

Atm	atmosphere
A_t	absorption at any time, t
A_e	absorption at the equilibrium position
A_o	absorption of the reactant
A_∞	absorption of the product
CH_3CN	acetonitrile
°C	degrees centigrade
cm	centimetres
CO	carbon monoxide
DMF	N,N-dimethylformamide
ΔH	enthalpy change for the reaction
°K	degrees Kelvin
K	equilibrium constant
k_1	kinetic rate constant
k_{-1}	kinetic rate constant
k_2	kinetic rate constant
k_{-2}	kinetic rate constant
k_f	overall rate constant for the forward reaction
k_r	overall rate constant for the reverse reaction
k obsd	pseudo-first-order rate constant
M	molarity
M(porp)L	five-coordinate metal porphyrin complex
$M(porp)L_2$	six-coordinate metal porphyrin complex
M(porp)(CO)L	carbonylated six-coordinate metal porphyrin complex
M(porp)LL'	mixed axial ligand six-coordinate metal porphyrin complex
Mp	mesoporphyrin IX dianion

min	minute
mL	millilitre
MS	mass spectrometry
μL	microlitre
N_2	nitrogen
n-Bu_3P	tri-n-butylphosphine
O_2	oxygen
OEP	octaethylporphyrin dianion
OMBP	octamethyltetrabenzoporphyrin dianion
Pc	phthalocyanine dianion
PpIX	protoporphyrin IX dianion
Py	pyridine
$Ru_3(CO)_{12}$	tri-ruthenium dodecacarbonyl
RuMb	ruthenium(II) reconstituted myoglobin
$RuMb^+$	ruthenium(III) reconstituted myoglobin
ΔS	entropy change for the reaction
sec	second
T	temperature
t	time
TBAB	tetrabutyl ammonium boranate
THF	tetrahydrofuran
TPP	tetraphenylporphyrin dianion
ε	molar extinction coefficient
ν	frequency

Acknowledgements

I would like to thank Drs. D. Dolphin and B.R. James for their supervision during the past few years, and also for their assistance in the production of this thesis. I also wish to thank M. Barley for his help in carrying out some experiments and for useful discussion. Thanks also to all my friends for assistance in proofreading and typing.

CHAPTER 1

INTRODUCTION

1.1 Decarbonylation of Aldehydes

The purpose of this chapter is to review the relevant literature on transition metal catalyzed decarbonylation reactions and some ruthenium porphyrin chemistry, especially that of ruthenium porphyrin phosphine systems.

The decarbonylations of aldehydes, acyl halides, aroyl halides and ketones are useful and important reactions in organic chemistry.[1-3] Transition metal complexes have been investigated for use as stoichiometric and catalytic decarbonylation agents, some of which, notably $RhCl(PPh_3)_3$, have been used for homogeneous decarbonylation.[4-9]

The $RhCl(PPh_3)_3$ complex acts as a stoichiometric homogeneous decarbonylation agent under mild conditions; the reactions with aldehydes, acyl, and aroyl halides are summarized by equation I.1.[4-8,10]

$$RCOX + RhCl(PPh_3)_3 \longrightarrow RX + \text{trans-}RhCl(CO)(PPh_3)_2 + PPh_3 \quad (X = H,Cl)$$

equation I.1

In the case of long chain aliphatic aldehydes some olefin is also produced, see equation I.2

$$RhCl(PPh_3)_3 + RCH_2CH_2CHO \longrightarrow RhCl(CO)(PPh_3)_2 + RCH_2CH_3 \text{ or } H_2 + RCH=CH_2$$

equation I.2

If a beta hydrogen is present similar reactions take place with acyl halides, in which case the only product of decarbonylation is olefin.[5]

The mechanism for decarbonylation of acid chlorides, proposed by Baird, Nyman and Wilkinson,[4] is shown in scheme I.1.[5,7,11-14] This mechanism has been supported by some kinetic data, and isolation of two intermediates, 2 and 3, in the case of R = aryl. The active intermediate is thought to be 1, which is formed as $RhCl(PPh_3)_3$ dissociates in solution.[11] This species is also thought to be important in the catalytic hydrogenation of olefins.[15,16]

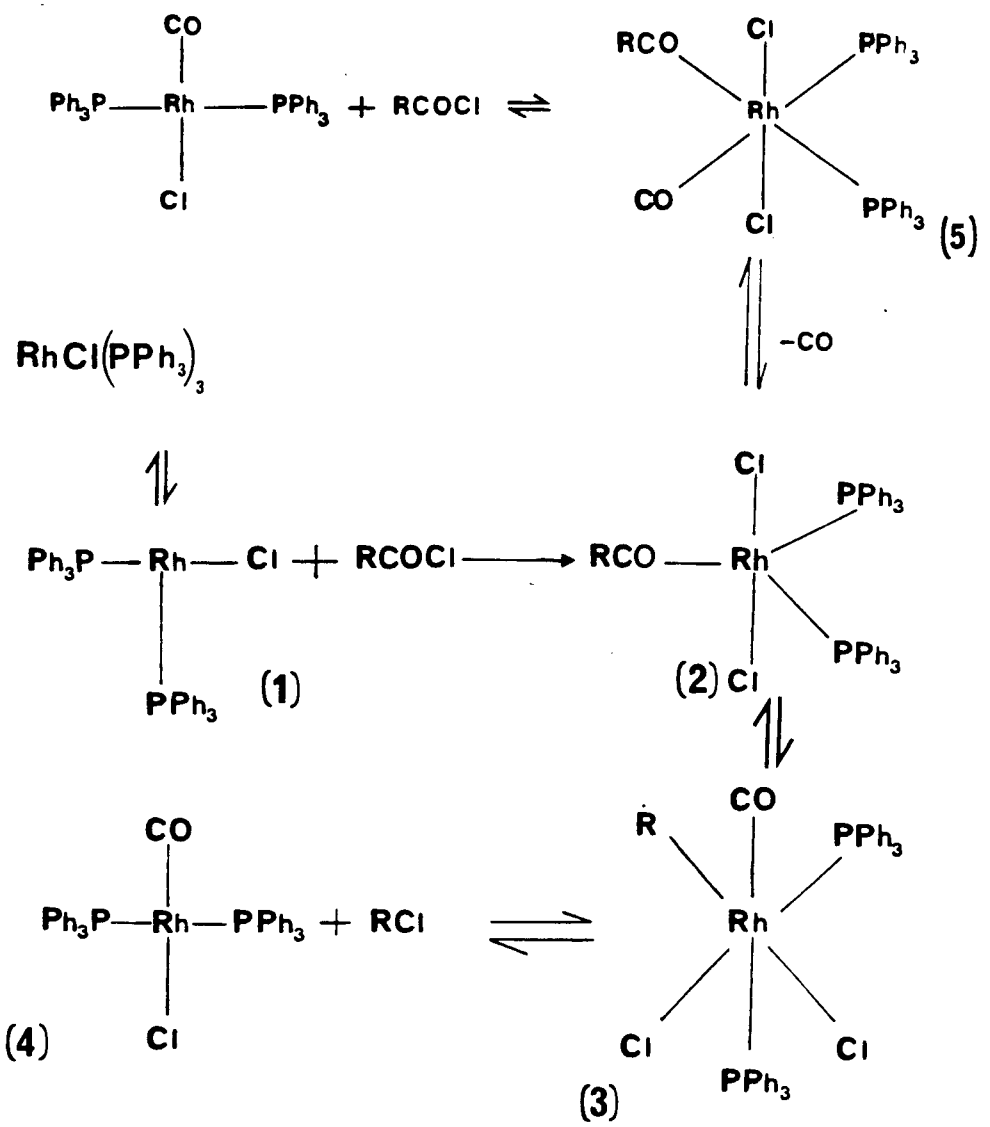

Scheme I.1. The Decarbonylation of Acyl Halides by $RhCl(PPh_3)_3$

The first step in the reaction is thought to be an oxidative addition to 1, to yield the five-coordinate acyl complex 2, which undergoes facile rearrangement to 3. The last step is a reductive elimination to yield 4, and alkyl halide.

This reaction, however, cannot be made catalytic at useful temperatures since the carbonyl complex formed is stable and does not lose CO even at high temperatures. An unsuccessful attempt was made to reverse the decarbonylation of $RhCl(CO)(PPh_3)_2$ (c.f. equation 1), in molten PPh_3.[17] Another approach was to regenerate the active complex by photolysis,[18] since many metal carbonyls dissociate CO in this way. However, photolysis of the carbonyl complex results in oxidation of the ligands, CO and PPh_3 to CO_2 and $P(Ph)_3O$, respectively, but the photoproduct obtained may be converted to $RhCl(PPh_3)_3$.[18] The photoproduct was not isolated but was thought to be an oxygen adduct, formed as a result of trace oxygen present during photolysis.

The decarbonylation of acid chlorides and aldehydes can be driven catalytically at very high temperatures. Ohno and Tsuji, among others, have used $RhCl(CO)(PPh_3)_2$ to catalytically decarbonylate several aroyl halides.[1,4,5,19] The first step is not the irreversible oxidative addition to form 2, but the formation of complex 5 (scheme I.1) which loses CO on heating to give the five-coordinate acyl complex. Although the catalytic decarbonylation using $RhCl(CO)(PPh_3)_2$ works smoothly for aryl compounds, giving up to 76% yield for cinnamaldehyde,[5] it was found that undesirable side reactions occurred when aliphatic aldehydes were used.

Most of the mechanistic work has been performed on acid halides, since no intermediates had been isolated for the corresponding aldehyde reactions. Recently, Suggs[20] has used a cyclometallation reaction, to isolate the generally unstable intermediate complexes thought to be

present in the decarbonylation of aldehydes. The acyl hydride, 6, obtained is the first such intermediate found and provides support for the mechanism discussed for decarbonylation of acyl halides.

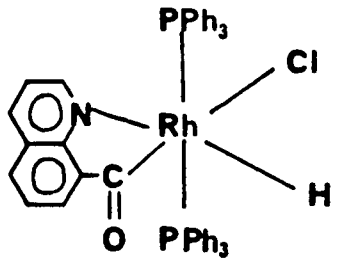

6

Rauchfuss has studied acyl complexes of metals, in view of their possible intermediacy in decarbonylation and other such reactions.[21] An unusual ruthenium complex, 7, which undergoes facile intramolecular decarbonylation, led him to postulate a mechanism involving a η^2(π-bonded) carbonyl, instead of the usual oxidative addition pathway. The rationale for this suggestion was based on the observation that ruthenium(IV) is not usually a readily attainable oxidation state.[22]

Other metal compounds have been employed as decarbonylation catalysts;[1] $PdCl_2$ has been used to decarbonylate substituted

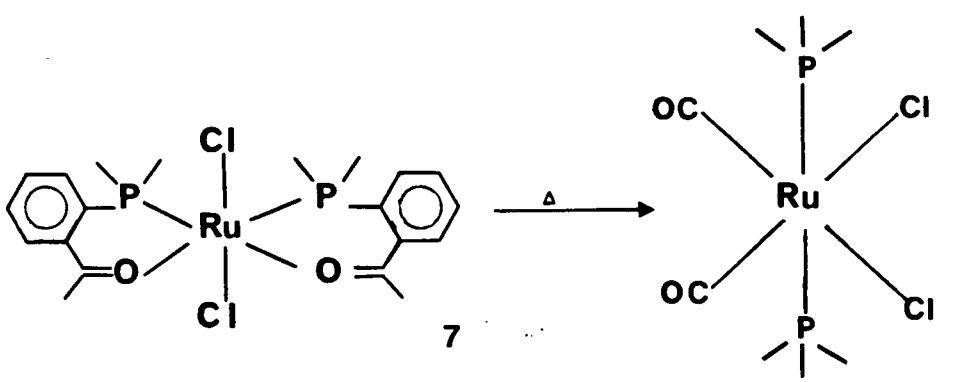

7

cinnamaldehydes in high yield.[23] Another palladium-based system using palladium metal catalytically converts myrtenal to apopinene.[24] The ruthenium complex, $\{Ru_2Cl_3[(C_2H_5)_2(C_6H_5)P]_6\}Cl$ has been studied as

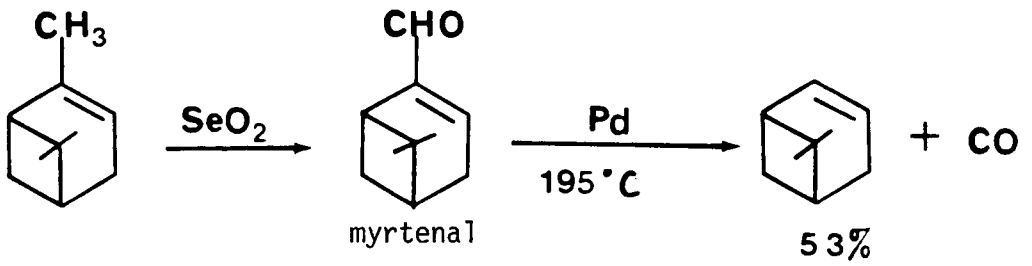

a stoichiometric decarbonylation agent.[1] However the major product in these cases is often olefin, and the hydrogen released reduces aldehyde to alcohol.

Recently a series of rhodium complexes have been shown to be useful decarbonylating catalysts, under relatively mild conditions, at 150°C.[25,26] The catalysts exhibit long term stability, high turnover numbers, and some selectivity. Mechanistic studies to date indicate that the oxidative addition step is the rate determining step. However, there is no direct evidence for Rh(III) intermediates. The other steps are the usual acyl-alkyl migration step, which obviously requires some rearrangement and opening of the chelate ligand and reductive elimination, see diagram on p. 6, although the full mechanistic details have not been elucidated as yet.

The temperature at which the catalyst operates is very important in decarbonylations, since at higher temperatures there are many side reactions which may occur; many aldehydes are known to undergo extensive thermal decomposition. A catalyst should also show some long term stability, measured by the total number of turnover numbers achieved.

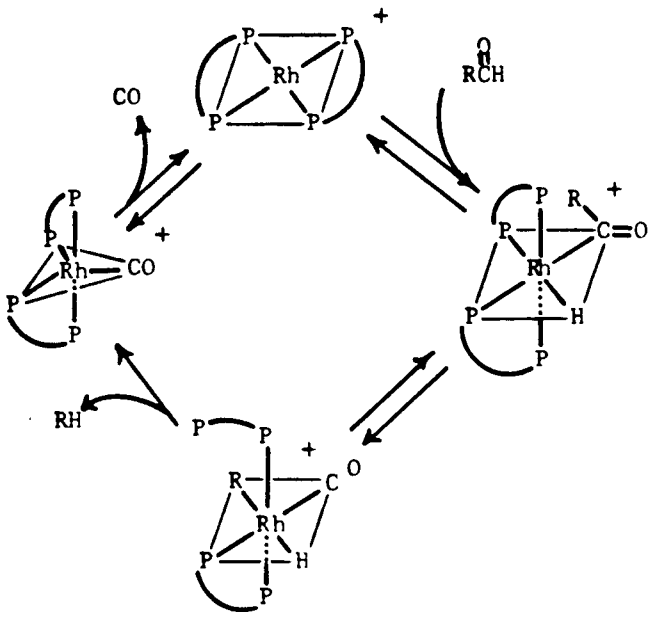

1.2 Ruthenium Metalloporphyrins

Until recently, interest in metalloporphyrin chemistry was based mainly on the biological significance of metalloporphyrins as the active sites in naturally occurring oxygen and electron transport systems, particularly those containing iron. However, recent studies have shown that, in addition to being good models for molecules such as haemoglobin and myoglobin, metalloporphyrins can also exhibit catalytic activity.[27,28] Several metalloporphyrins catalyze oxidations using oxygen,[27] while some cobalt porphyrins have recently been shown to electrocatalytically reduce oxygen to water.[28,29] A Ru(II) porphyrin system has also been found to catalytically decarbonylate aldehydes.[30] Furthermore, although simple Fe(II) porphyrin systems are not stable to autoxidation, it was anticipated that the Ru(II) analogues, being more substitution-inert, would not oxidize so readily and might thereby facilitate the study of oxygen activation.

In the early seventies the first reports appeared on the synthesis and characterization of some Ru(II) porphyrins.[31] The general synthetic

route, using $Ru_3(CO)_{12}$, and the free base of the porphyrin, leads to the formation of a monocarbonyl.[32]

$$Ru_3(CO)_{12} + H_2P \xrightarrow{EtOH} RuP(CO)(EtOH)$$

(P = OEP, TPP, MpIX)

equation I.3

The enhanced lability of axial ligands in metalloporphyrin complexes, compared to related octahedral non-porphyrin systems, is demonstrated by the extensive chemistry of these bis-ligand species, scheme I.2.[33] Unlike the corresponding Fe(II) systems the $Ru(porp)L_2$ species are generally air-stable in the solid state, although oxidation to Ru(III) can occur in solution. Following the reported reactivity of

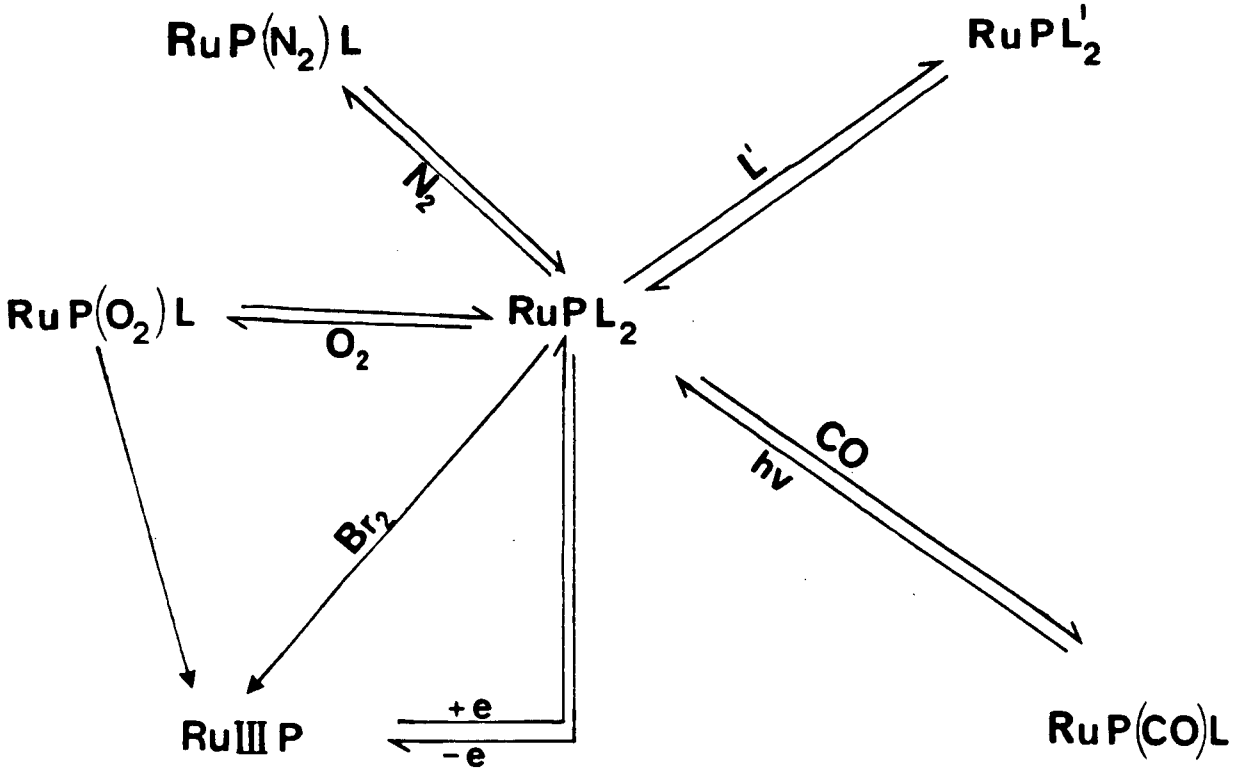

Scheme I.2. The Chemistry of $RuPL_2$ Species

$Fe(porp)L_2$ with oxygen at low temperatures, to give the oxygen adduct,[34] studies were initiated in this laboratory on the reactivity of $Ru(porp)L_2$ with O_2, at both sub-zero and ambient temperatures. It was discovered that $RuOEP(CH_3CN)_2$ in DMF or pyrrole solution, absorbed 1 mole of O_2 per ruthenium atom, at ambient temperatures.[35] In addition to binding O_2 reversibly the complex also bound CO to form the monocarbonyl.[35]

Some preliminary kinetic data for the reaction with O_2 was analyzed for a dissociative mechanism, like a corresponding Fe(II) system[36-38] as shown in equation I.4

$$M(porp)L_2 \underset{+L}{\overset{-L}{\rightleftharpoons}} M(porp)L \underset{-X}{\overset{+X}{\rightleftharpoons}} M(porp)(X)(L)$$

$$(X = O_2, CO)$$

equation I.4

The oxygen adduct, $Ru(porp)(O_2)(L)$, was not isolated, as oxidation to Ru(III) occurred during the work-up procedure.[35] Thus the nature of the RuO_2 bond remains uncertain. Initially a $Ru(III)\text{-}O_2^-$ superoxide formulation was favoured, as polar aprotic solvents, which would tend to stabilize such a charge-separated species, enhanced oxygenation.[39] The absence of an e.s.r. signal also indicated Ru(III) formation. Other evidence suggested a peroxoruthenium(IV) system,[39] although Ru(IV) is a rare oxidation state.

Following the success in reacting O_2 with $RuOEP(CH_3CN)_2$ and $RuMpIX(DMF)_2$, it was anticipated that reconstituted myoglobin, RuMb, might bind O_2. However, treatment of RuMb with O_2 in phosphate buffer at 0°C gave only irreversible oxidation to $RuMb^+$.[40] The mechanism involved is thought to be an outer sphere oxidation of a six-coordinate moiety, within the protein.

An important feature of some $Ru(porp)L_2$ complexes, initially noted by Chow and Cohen,[31a] was their ability to abstract CO from organic substrates. These workers found that $RuTPP(aniline)_2$ in refluxing acetic anhydride formed RuTPP(CO)(aniline). Subsequently, during the preparation of $RuMpIX(DMF)_2$, which involved prolonged photolysis of RuMpIX(CO)(EtOH) in DMF, catalytic decarbonylation of the solvent occurred.[40]

$$Ru(porp)(DMF)_2 \longrightarrow Ru(porp)(CO)DMF + HNMe_2$$

$$\uparrow \quad h\nu, DMF \quad \downarrow$$

Other $Ru(porp)L_2$ species exhibited strong affinities for CO. Kinetic studies on $RuOEP(CH_3CN)_2$ in toluene at 30°C, yielded an equilibrium constant K, of ca. 10^4, for the reaction with CO to give $RuOEP(CO)(CH_3CN)$.[41] These observations led us to attempt development of a photocatalytic system using $Ru(porp)L_2$ for the decarbonylation of aldehydes. Initially, the stoichiometric reaction of $RuOEP(CH_3CN)_2$ with phenylacetaldehyde was investigated. The CO abstraction was rapid, but attempts to make the reaction photocatalytic were unsuccessful, as small excesses of acetonitrile, which seemed to be essential for the photochemical loss of CO from the ruthenium carbonyl, inhibited the reaction.

Another approach to a catalytic decarbonylation, is to somehow labilize the CO of the metal carbonyl adduct, as the main problem in the catalytic cycle is the removal of CO from the adduct formed, e.g. as in the $RhCl(PPh_3)_3$ system (see above). Until recently the carbonyl in Ru(porp)(CO)(L) has been considered relatively non-labile, although photolysis in the presence of excess ligand, L, was known to regenerate the $Ru(porp)L_2$ species.[42] However, some phosphine ligands have been

shown to thermally displace CO from Ru(porp)(CO)(EtOH), leading to Ru(porp)(phosphine)$_2$ complexes.[43] The ligands tri-n-butylphosphine and $PPh_2CH_2PPh_2$, for example, readily displace CO from both the OEP and TPP complexes, whereas triphenylphosphine will displace CO from TPP complexes only, and that requires prolonged heating with a large excess of phosphine.[44] Tri-n-butylphosphine, in contrast, rapidly forms the bis phosphine complex using a small excess, at ambient temperatures.

The porphyrin phosphine systems were reactive towards several small gas molecules, such as O_2, CO, SO_2, N_2, and were also investigated as potential decarbonylation catalysts.[30] RuTPP$(PPh_3)_2$, which dissociates a phosphine ligand rapidly in solution, catalytically decarbonylated phenylacetaldehyde in CH_2Cl_2 at ambient temperatures, but the system was inefficient, and yielded low turnover numbers.

The objective of the work was to design a complex which would (i) abstract CO from aldehydes and (ii) form a carbonyl adduct containing a labile CO. Tri-n-butylphosphine not only displaces CO readily from Ru(porp)(CO)(EtOH) but also, being a good π-acceptor, labilizes a trans CO, Chapter 3. This increased lability is possibly reflected in the νCO values for the monocarbonyl complexes, see Table I.1. RuTPP(CO)(n-Bu_3P) has a CO frequency significantly higher than the triphenylphosphine analogue, implying less back-bonding in the butyl system. Based on such factors, a small excess of tri-n-butylphosphine was added to a solution of RuTPP$(PPh_3)_2$ in dichloromethane and acetonitrile in an attempt to find an effective catalytic decarbonylation system. It has been reported previously that nitrile solvents have a stabilizing effect on intermediate species in some rhodium catalyzed decarbonylations.[1] This system, RuTPP$(PPh_3)_2$/tri-n-butylphosphine, in CH_2Cl_2/CH_3CN, was found to catalytically decarbonylate several

Table I.1. ν(CO) Values in cm^{-1} for Various Ru(II) Porphyrins[44]

COMPOUND	ν(CO) SOLID[c]	ν(CO) SOLUTION
RuOEP(CO)(EtOH)	1928	1928[a]
RuOEP(CO)(py)	1939	
RuOEP(CO)(PPh_3)	1954	1953[a]
RuOEP$(CO)_2$	1990	
RuTPP(CO)(py)	1943	
RuTPP(CO)[$(p\text{-}MeOPh)_3P$]	1950	
RuTPP(CO)(PPh_3)	1956	
RuTPP$(CO)_2$	2005	
RuTPP(CO)($n\text{-}Bu_3P$)		1980[b]
RuOEP(CO)(Cy_3P)		1935[a]

[a] In $CHCl_3$.
[b] In CCl_4.
[c] Solid deposited on NaCl plates.

aldehydes at ambient temperatures. Details of this catalytic system are discussed in Chapter 4.

The reactions of RuTPP$(n\text{-}Bu_3P)_2$ with CO gas (Chapter 3) and phenylacetaldehyde (Chapter 5) have been studied with a view to elucidation of the mechanism of decarbonylation. Kinetic parameters have been obtained for the reaction with CO.

CHAPTER 2

EXPERIMENTAL

2.1 General Methods

2.1.1 Elemental Analysis

Microanalyses were carried out by Mr. P. Borda of this department.

2.1.2 Gas-Liquid Chromatography

Gas liquid chromatography was performed on a Hewlett-Packard 5830A or a Carle 113 instrument, using OV101 and OV17 columns.

2.1.3 Visible Spectrometry

Visible spectra were recorded on a Cary (Model 17) spectrometer, fitted with a thermostated cell compartment for kinetic studies. Quartz cells of path length 1 cm were used.

2.1.4 Mass Spectrometry

Mass spectra were recorded on a Varian MAT CH or a KRATOS/AEI MS-902. GLC mass spectrometry was carried out on a VG Micromass 12 instrument.

2.1.5 Infra-Red Spectroscopy

All infra-red spectra were recorded on a Perkin-Elmer 457 grating spectrophotometer calibrated with polystyrene.

2.1.6 Cyclic Voltammetry

Cyclic voltammetry was performed in a H cell and potentials were measured at a Pt electrode against a Ag/AgCl reference electrode.

2.1.7 Photolysis

Photolyses were performed using a 600 D Bl-PIN tungsten halogen lamp.

2.1.8 Gases

Purified argon was supplied by Canadian Liquid Air Ltd. and used without further purification. C.P. grade carbon monoxide was obtained from Union Carbide.

2.1.9 Solvents

All solvents were distilled under an inert atmosphere, and handled under argon using Schlenk techniques.[45] Dichloromethane (spectral grade) was distilled from CaH_2, as was acetonitrile (Burdick and Johnson, distilled in glass). Toluene (Fisher Scientific Co., spectral grade) was distilled from sodium-potassium amalgam. Benzene (Eastman Kodak, spectral grade) was distilled from sodium benzophenone ketyl.

2.1.10 Materials

All aldehydes were repeatedly distilled, usually under vacuum. Tri-n-butylphosphine was also distilled several times under vacuum. Both aldehydes and phosphine were stored under argon.

2.1.11 Nuclear Magnetic Resonance Spectroscopy

Proton n.m.r. spectra were recorded at 270 MHz with a U.B.C. N.M.R. centre modified Nicolet-Oxford M-270 spectrometer. Tetramethylsilane was used as internal standard.

2.2 Decarbonylation Procedure

A few milligrams of $RuTPP(PPh_3)_2$ were dissolved in CH_2Cl_2 under argon, and to this were added 10-25 mL of CH_3CN, making up a solution of

ca. 10^{-4} molarity. A small amount of CO was blown over the solution forming RuTPP(CO)(PPh_3), characterized spectrophotometrically (addition of excess substrate at this stage also generates the carbonyl complex). The solution was stirred continuously under argon, and samples were withdrawn using syringes and analyzed by GLC. Variations of this experimental procedure were also tried in an attempt to study the reaction more systematically, since reactivity tended to be irreproducible. Some solutions were degassed prior to addition of aldehyde, and CO was not admitted to the system; in these cases the aldehyde served as a source of CO, to produce RuTPP(CO)(PPh_3). As usual 5-10 μL of tri-n-butylphosphine were added and argon was blown through the solution. Products were collected in a cold trap, using a hexane-liquid nitrogen slush. Unfortunately this type of procedure was not convenient with volatile solvents, such as CH_3CN, and in some cases benzonitrile was substituted.

2.3 Spectrophotometric Kinetic Measurements

Due to the sensitivity of certain materials (solutions of the porphyrin complexes, aldehyde substrates etc.) used, and also the nature of the experiment, all optical density measurements were carried out in an evacuable cell, Fig. II.1. The cell was maintained at constant temperature by placing it in a thermostated cell compartment, which was attached to a Tanson circulating bath.

In a typical run using CO gas, a solution of the ruthenium complex was placed in the bulb (B) and degassed by three freeze-pump-thaw cycles. The cell was placed in the thermostated compartment for approximately 30 min to equilibrate in vacuo. After the initial spectrum was recorded, a known pressure of gas was admitted to the cell, which was shaken vigorously to ensure complete mixing of gas in solution. The corresponding

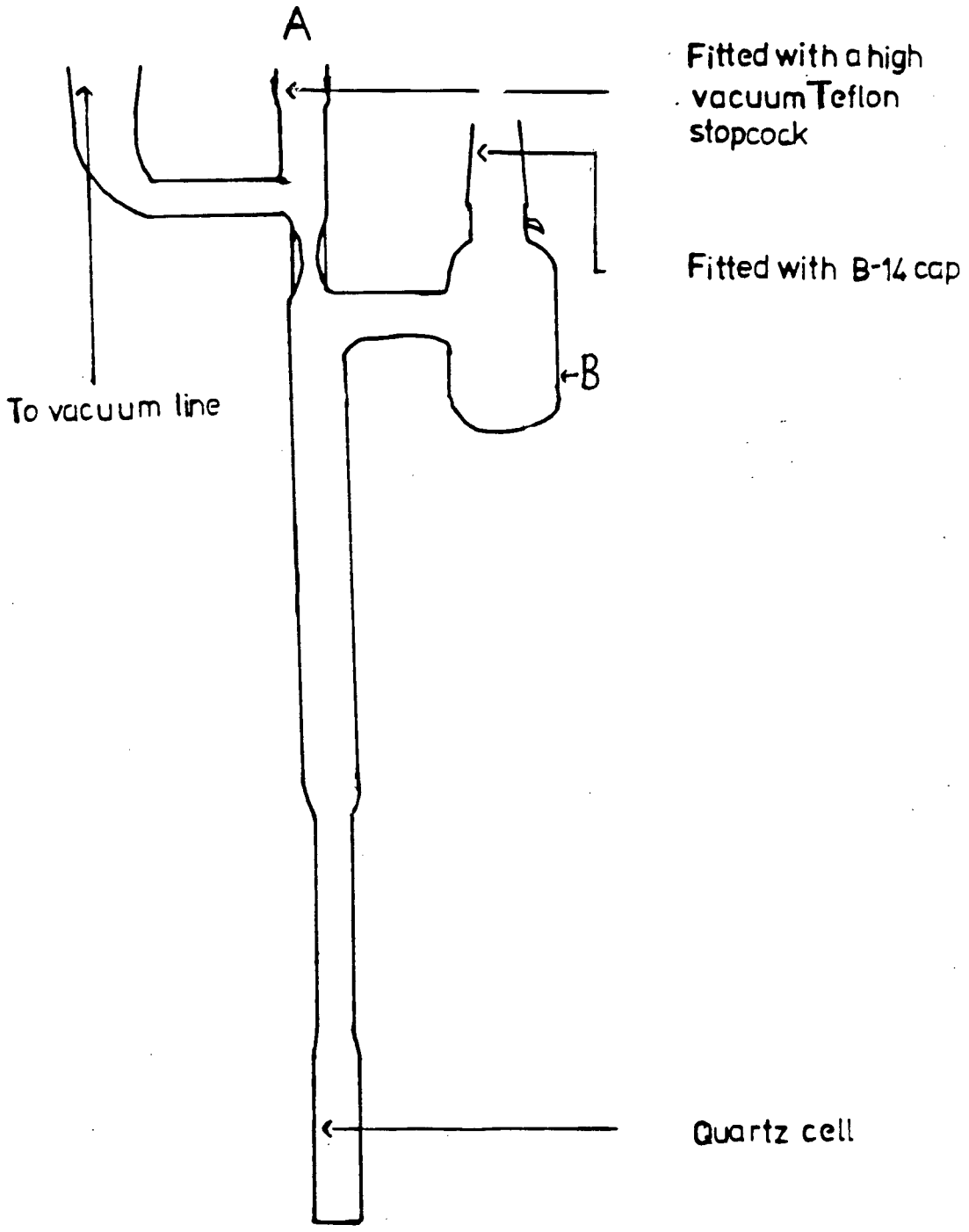

Figure II.1. Evacuable Cell for Optical Density Measurements

carbonylation reaction was then monitored to completion. Since the concentrations of the complexes used were low (of the order of $2\text{-}8\times10^{-5}$M) and the solubility of carbon monoxide is approximately 6×10^{-3}M atm^{-1}, the gas concentrations in solution, and the partial pressure of the gas above the solution were assumed to remain constant throughout any one experiment. The pressure of the gas was measured using a mercury manometer.

2.4 Complexes

Carbonyl(ethanol)octaethylporphyrinatoruthenium(II)

RuOEP(CO)(EtOH) was prepared by a method similar to that of Tsutsui et al.,[31b] as described in a previous thesis from this laboratory.[41]

Analysis: calculated for $C_{39}H_{50}N_4O_2Ru$: C, 66.19%; H, 7.07%; N, 7.92%. Found: C, 66.13%; H, 7.18%; N, 7.86%.

Visible Spectrum: λ_{max} in nm: 549, 518, 395, 375 (sh). log ε: 4.35, 4.12, 5.25.

Bis(acetonitrile)octaethylporphyrinatoruthenium(II)

RuOEP$(CH_3CN)_2$ was prepared by a general method described by Whitten et al.[43]

Analysis: calculated for $C_{40}H_{50}N_6Ru$: C, 67.13%; H, 6.99%; N, 11.75%. Found: C, 67.50%; H, 6.94%; N, 11.63%.

Visible Spectrum: λ_{max} in nm: 528, 496, 405, 374 (sh), 385 (sh). log ε: 4.23, 4.02, 5.34.

Bis(tri-n-butylphosphine)tetraphenylporphyrinatoruthenium(II)

RuTPP$(n\text{-}Bu_3P)_2$ was prepared by adding an excess of tri-n-butylphosphine (3×10^{-2} moles) to a 10^{-4}M solution of RuTPP$(PPh_3)_2$ in CH_2Cl_2-MeOH (4:1, v/v) at room temperature. The dichloromethane was removed slowly using N_2 and the complex crystallized out of MeOH. The crystals were

washed with cold hexane and dried in vacuo.

Analysis: calculated for $C_{68}H_{82}N_4P_2Ru$: C, 73.02%; H, 7.39%; N, 5.03%. Found: C, 73.00%; H, 7.25%; N, 4.84%.

Visible Spectrum: λ_{max} in nm: 560, 527, 437. log ε: 4.01, 4.17, 5.30.

Bis(triphenylphosphine)tetraphenylporphyrinatoruthenium(II)

$RuTPP(PPh_3)_2$ was prepared by a method described previously.[44,45]

Analysis: calculated for $C_{80}H_{58}N_4P_2Ru$: C, 77.59%; H, 4.72%; N, 4.52%. Found: C, 77.22%; H, 4.78%; N, 4.36%.

Visible Spectrum: λ_{max} in nm: 550, 515.7, 435, 413.3. log ε: 3.38, 3.74, 5.02, 4.41.

Carbonyl(tri-n-butylphosphine)tetraphenylporphyrinatoruthenium(II)

$RuTPP(CO)(n\text{-}Bu_3P)$ was prepared by bubbling CO through a solution of $RuTPP(n\text{-}Bu_3P)_2$ (10^{-4}M) in ca. 25 mL CH_2Cl_2-MeOH (5:1, v/v). The product was crystallized out of cooled methanolic solution after removal of CH_2Cl_2 by vaporization. The product was washed with cold methanol and dried in vacuo.

Analysis: calculated for $C_{57}H_{55}N_4OPRu$: C, 72.65%; H, 5.87%; N, 5.96%. Found: C, 68.46%; H, 5.60%; N, 5.39%.

Visible Spectrum: λ_{max} in nm: 581, 542, 420. log ε: 3.96, 4.17, 5.50.

Mass Spectrometry: m/e values: 916 $(M\text{-}CO)^+$, 714 $(RuTPP)^+$.

Both the mass spectrum and visible spectrum obtained indicate that the compound is indeed as formulated. However, the analyses indicate that some impurity may be present in the crystals. At first it was suspected that some solvent, probably methanol, had crystallized with the solid complex. The i.r. and ^1H n.m.r. spectra showed no peaks due to free methanol or dichloromethane.

The pattern of peaks in the n.m.r. spectrum suggests that two phosphine complexes are present in solution. The main set of peaks at +0.30 δ (P-$(CH_2)_2\underline{CH_2}\underline{CH_3}$), -1.45 δ (P-$CH_2\underline{CH_2}CH_2CH_3$) and -2.70 δ (P-$\underline{CH_2}(CH_2)_2CH_3$) are assigned to the RuTPP(CO)(n-Bu_3P) complex by comparison with the spectrum of RuOEP(CO)(n-Bu_3P).[44] Another set of peaks occur at +0.36 δ, -1.14 δ and -2.28 δ. These are assigned to the bis phosphine complex, RuTPP(n-$Bu_3P)_2$. This was confirmed by comparison with the n.m.r. of an authentic sample of RuTPP(n-$Bu_3P)_2$.

The starting material, RuTPP(n-$Bu_3P)_2$ is not likely to be the impurity giving rise to the poor analysis, since the percentage carbon of the two compounds is so close, see above. The impurity is probably some excess n-Bu_3P which, in concentrated solutions of the complexes, would easily displace CO from RuTPP(CO)(n-Bu_3P) forming RuTPP(n-$Bu_3P)_2$.

CHAPTER 3

THE REACTION OF RuTPP(n-$Bu_3P)_2$ AND CO

3.1 Spectral Characteristics

Toluene was used as a solvent to study this reaction, for the sake of comparison with previous studies. On addition of about one atmosphere of CO to a solution of RuTPP(n-$Bu_3P)_2$, a series of spectral changes was observed as a function of time. There were several clean isosbestic points and the reaction appeared to go to completion, forming RuTPP(CO)(n-Bu_3P), judging by the spectral changes (see Figure III.1). To establish pseudo-first-order conditions with respect to phosphine concentrations, small amounts of tri-n-butylphosphine were added to the solutions prior to reaction with CO. In order to follow the rate of reaction successfully the excess phosphine used was less than twenty-fold since an equilibrium is set up according to the following equation.

$$RuTPP(n\text{-}Bu_3P)_2 \underset{\longleftarrow}{\overset{+CO}{\longrightarrow}} RuTPP(CO)(n\text{-}Bu_3P) + n\text{-}Bu_3P$$

equation III.1

The position of the equilibrium obtained is dependent on the CO pressure used and the amount of excess phosphine added. At pressures of CO less than one atmosphere, with no excess phosphine, the reaction again did not go to completion. This is in contrast to the analogous OEP system,[41] where the reaction went to completion under all pressures of CO, down to about 0.21 atmospheres.

Figure III.2 shows typical spectral changes characteristic of the reaction (the Soret bands are not shown, as they are off the scale at the concentrations used). As with the RuOEP(n-$Bu_3P)_2$ system, excess

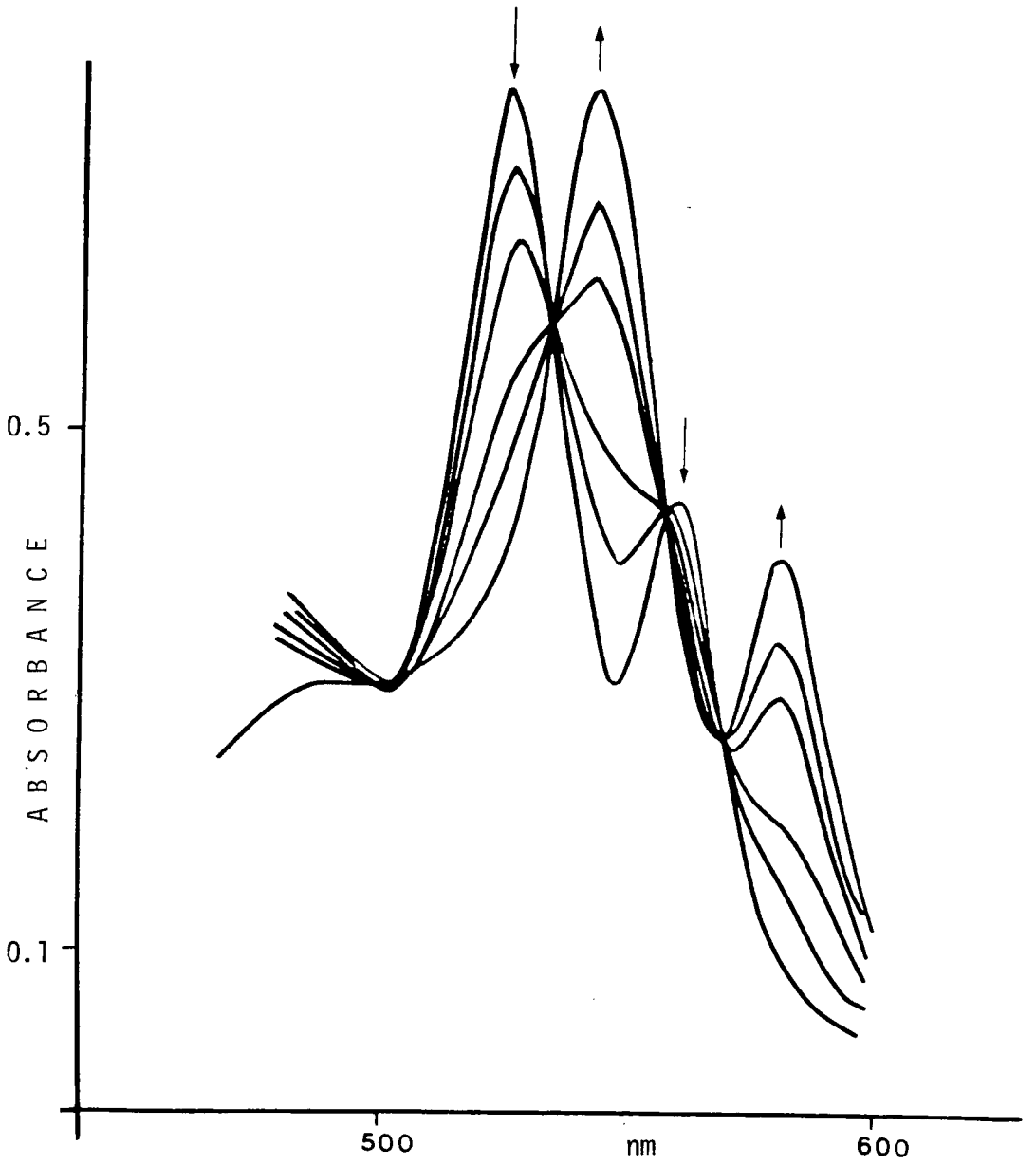

Figure III.1. Spectral Changes for the Reaction of CO with $RuTPP(n\text{-}Bu_3P)_2$ in Toluene at 26°C with No Added Phosphine

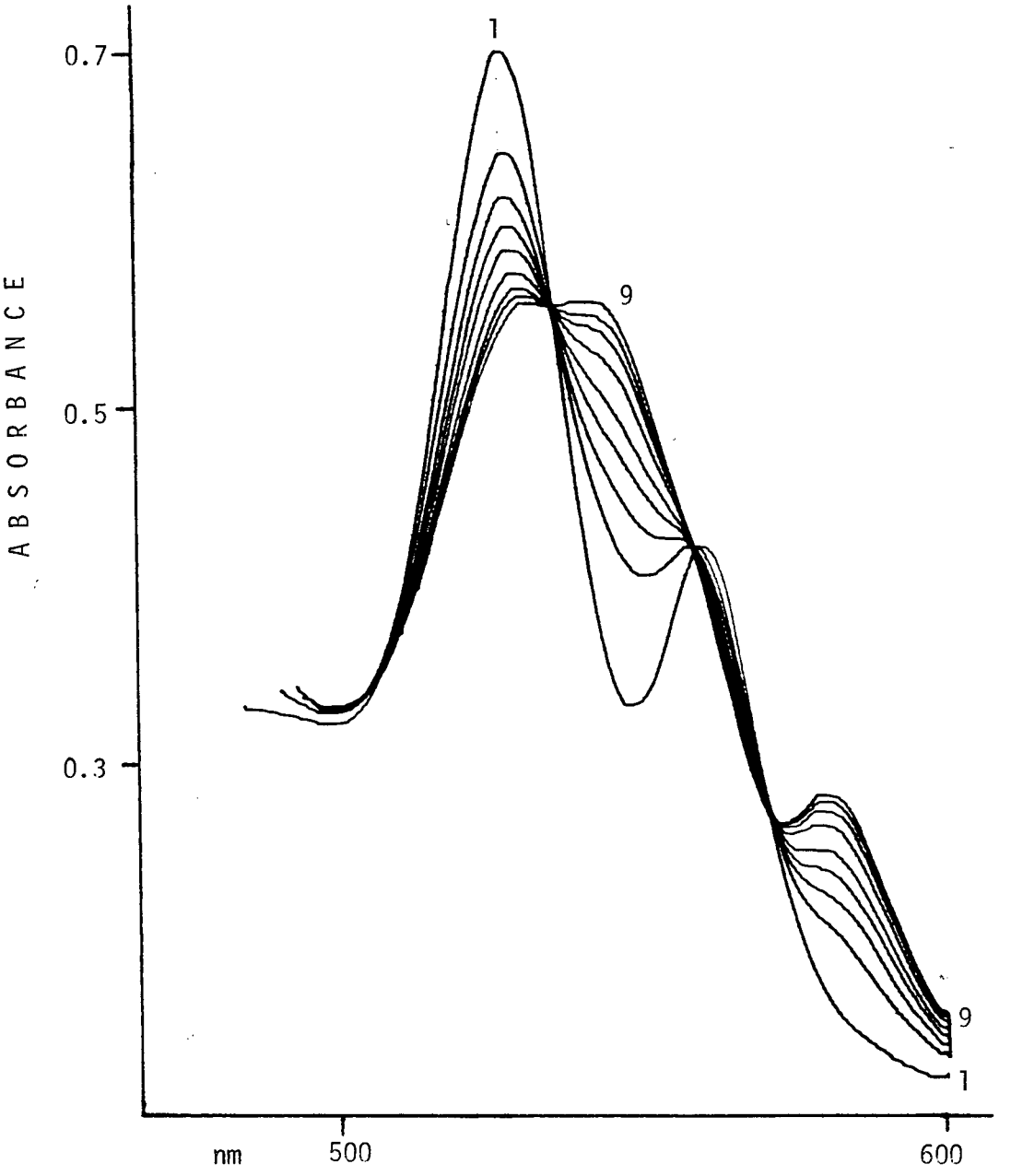

Figure III.2. The Reaction of $RuTPP(n\text{-}Bu_3P)_2$ with 1 atm of CO in Toluene at 1.67×10^{-4} M Phosphine

phosphine is not necessary to generate the correct spectrum for six-coordinate species. In the initial spectrum of RuTPP(n-$Bu_3P)_2$, there are bands at 560nm (log ε = 4.01), 527nm (log ε = 4.17), and 437nm (log ε = 5.30). The spectrum of RuTPP(CO)(n-Bu_3P) has bands at 581nm (log ε = 3.96), 542nm (log ε = 4.17) and 420nm (log ε = 5.50).

The latter are determined from spectral data using one atmosphere of CO, when it is assumed that the reaction has gone to completion. At any equilibrium position, bands of both starting complex and carbonylation product were present. Reaction times varied from 25 min to 90 min, depending on temperature and concentration of ligands.

3.2 Treatment of Data

The kinetic data were obtained by following the decrease in spectral intensity of the 527nm band of the bis-phosphine complex. Plots of $\log\left(\frac{A_t-A_e}{A_o-A_e}\right)$ versus time gave good straight lines, Figure III.3. A_e is the absorbance at equilibrium and A_t is the absorbance at any time, t, during the reaction and A_o is the absorbance at t = 0. This demonstrates that the reaction follows pseudo-first-order kinetics under the conditions of the experiment. The CO concentration is much larger (about 10^2 times) than that of the porphyrin. The overall variation in the spectral changes of the reaction with CO pressure and phosphine concentration is consistent with the simple one-to-one equilibrium shown in equation III.1, for which

$$K = \frac{[\text{RuTPP(CO)(n-Bu}_3\text{P)}]\ [\text{n-Bu}_3\text{P}]}{[\text{RuTPP(n-Bu}_3\text{P)}_2]\ [\text{CO}]}$$

This can be written as

$$\log K = \log\ [A_o-A_e/A_e-A_\infty] - \log[CO] + \log[Bu_3P]$$

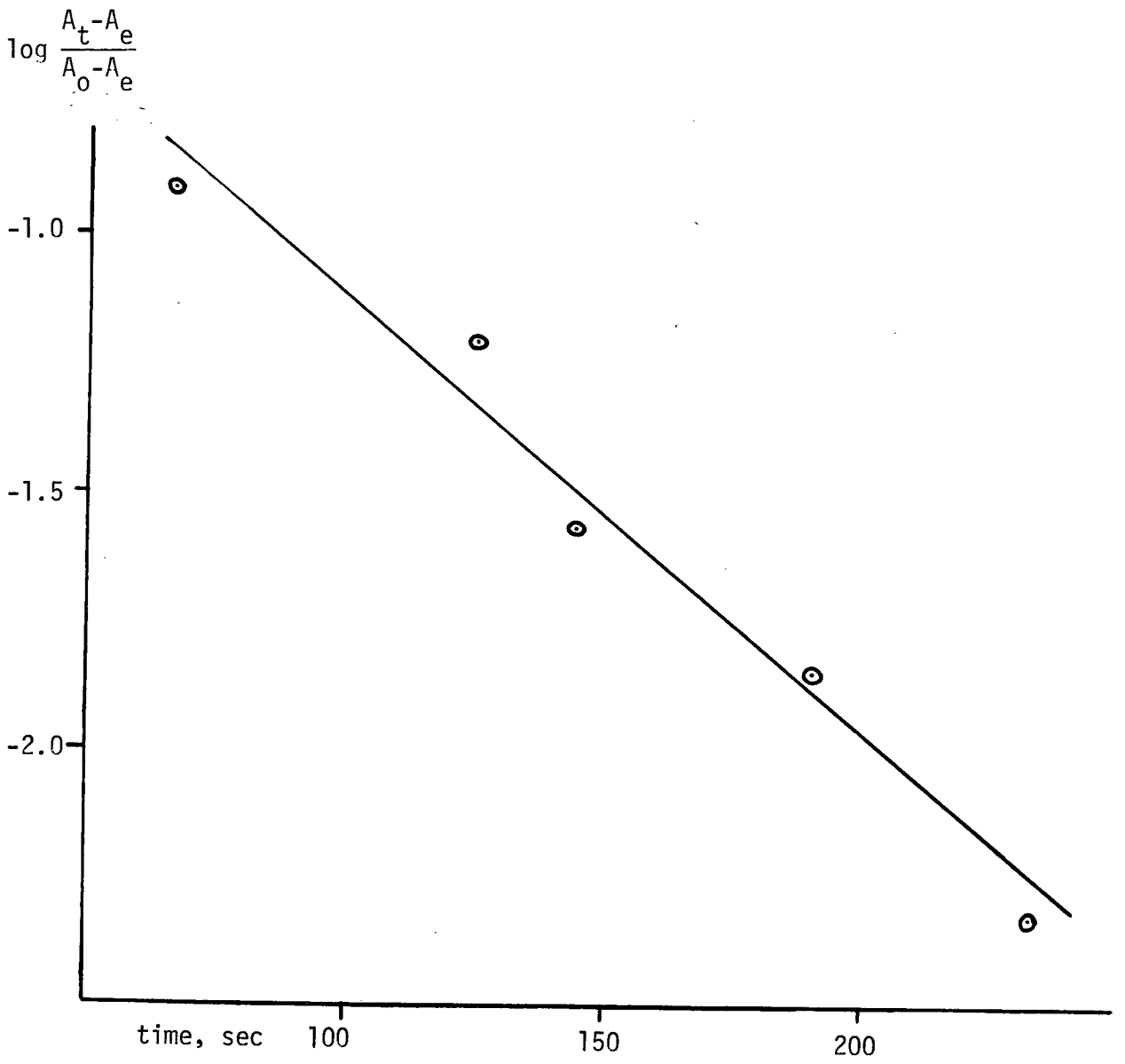

Figure III.3. First Order Plot for the Reaction of $RuTPP(n\text{-}Bu_3P)_2$ with CO in Toluene at 31°C

where, A_o = absorbance of $RuTPP(n\text{-}Bu_3P)_2$, and A_∞ = absorbance of product, estimated by extinction coefficients and A_e = absorbance at equilibrium. The CO pressure is converted to molarity using the known solubility of CO in toluene.[46]

The equilibrium constants were calculated from plots of log $A_o\text{-}A_e/A_e\text{-}A_\infty$ versus log $[n\text{-}Bu_3P]$, at a fixed CO pressure. In all cases straight line plots of slope = -1.0 ± 0.15 were obtained (Figure III.4). The K values thus obtained are listed in Table III.1. A plot of ln K versus 1/T (Figure III.5) gave a good straight line from which the following thermodynamic parameters were obtained;

$$\Delta S° = 78.9J/deg \pm 20J/deg \quad \Delta H° = 30.5kJ \pm 4kJ.$$

Table III.1. Equilibrium Constants for the Reaction of $RuTPP(n\text{-}Bu_3P)_2$ with CO at Different Temperatures

Temp. °C	21	26	31	36	41
K	0.049	0.054	0.068	0.083	0.107

Some individual rate constants were also calculated, assuming that the mechanism corresponds to that of the $RuOEPL_2$ (where L = $n\text{-}Bu_3P$, or CH_3CN) systems, i.e. a dissociative mechanism, equation III.2.

$$RuTPP(n\text{-}Bu_3P)_2 \underset{k_{-1}}{\overset{k_1}{\rightleftharpoons}} RuTPP(n\text{-}Bu_3P) \underset{k_{-2}}{\overset{k_2}{\rightleftharpoons}} RuTPP(CO)(n\text{-}Bu_3P).$$

equation III.2

Since an equilibrium exists, k_{-2} cannot be assumed to be negligible, and the rate law becomes

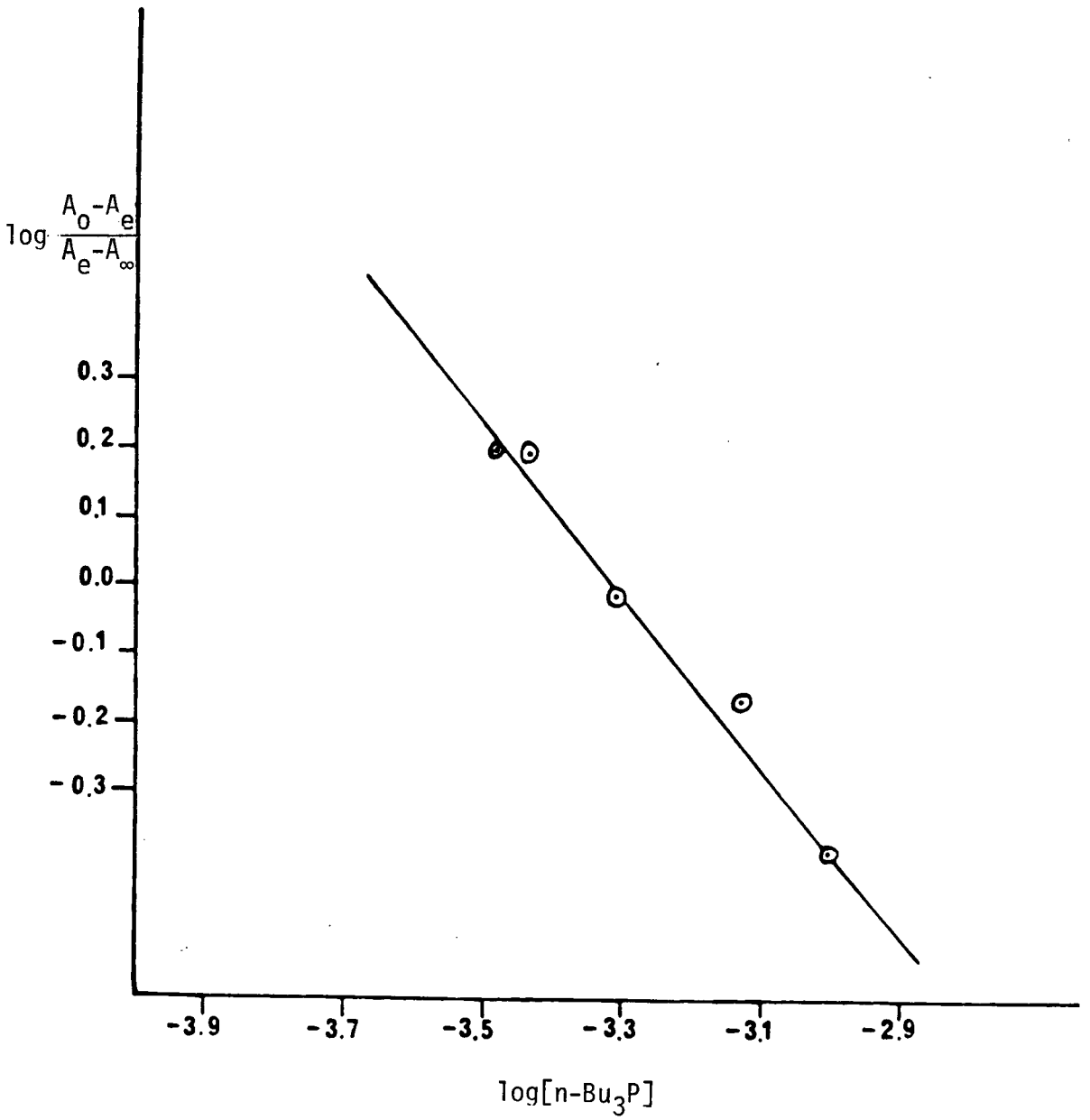

Figure III.4. Log A_o-A_e/A_e-A_∞ Versus [n-Bu_3P] at Constant CO Pressure

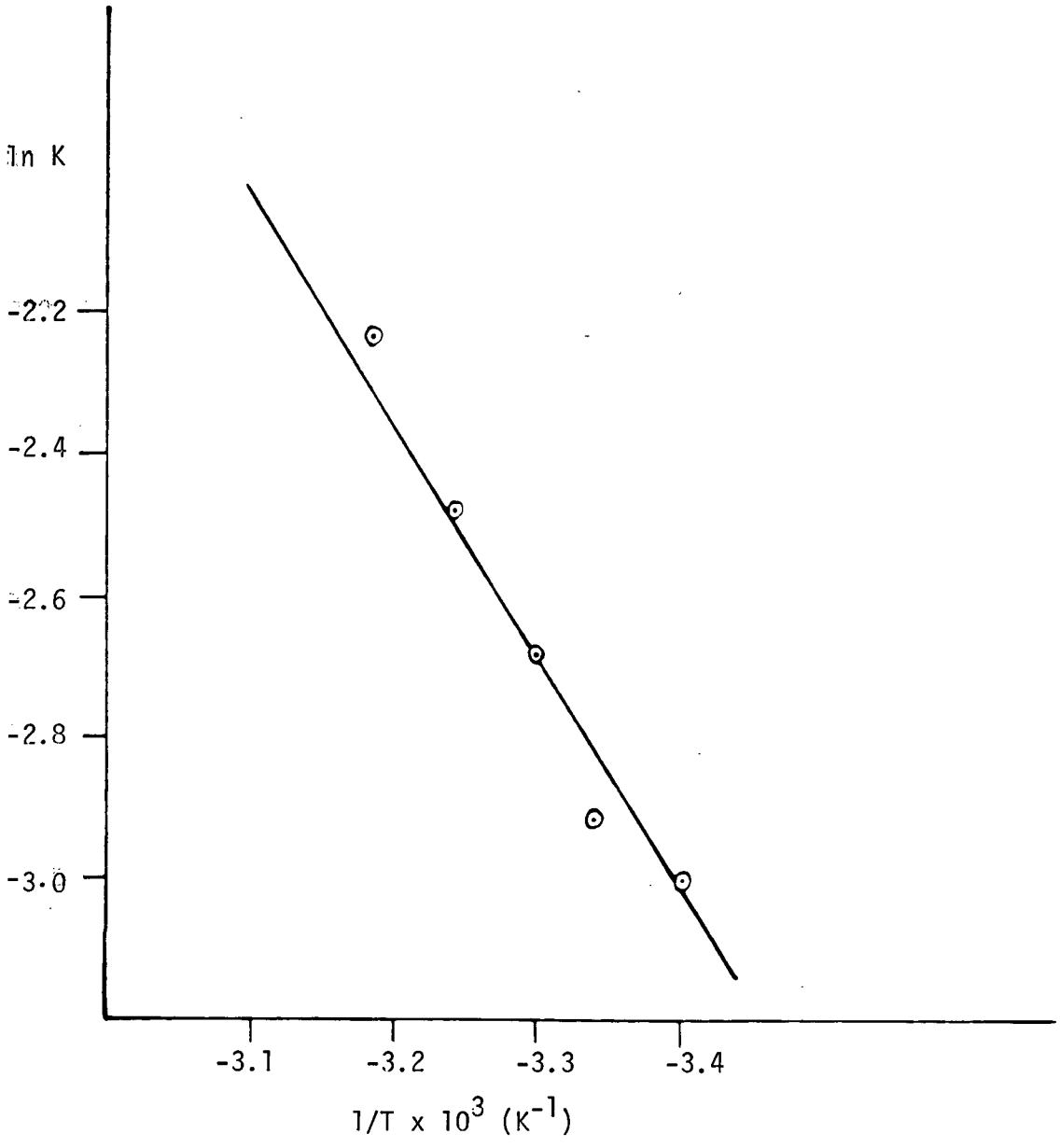

Figure III.5. Van't Hoff Plot for the Reaction of $RuTPP(n\text{-}Bu_3P)_2$ with CO in Toluene

$$\text{rate} = \frac{k_1 k_2[CO]\,[RuTPP(n\text{-}Bu_3P)_2]}{k_{-1}\,[n\text{-}Bu_3P] + k_2[CO]} - \frac{k_{-1}k_{-2}[n\text{-}Bu_3P]\,[RuTPP(CO)(n\text{-}Bu_3P)]}{k_{-1}\,[n\text{-}Bu_3P] + k_2[CO]}$$

which can be rewritten,

$$\text{rate} = k_f[RuTPP(n\text{-}Bu_3P)_2] - k_r[RuTPP(CO)(n\text{-}Bu_3P)]$$

where k_f is the overall pseudo-first-order rate constant for the forward reaction and k_r is the overall pseudo-first-order rate constant for the reverse reaction. The CO and phosphine concentrations remain constant during one experiment. This expression can now be integrated[47] to give

$$(k_f + k_r)t = \ln A_o\text{-}A_e/A_t\text{-}A_e,$$

A_e = absorbance at equilibrium

A_t = absorbance at any time, t

A_o = absorbance of initial $RuTPP(n\text{-}Bu_3P)_2$.

Plots of $\ln A_o\text{-}A_e/A_t\text{-}A_e$ versus time, gave good straight lines of

$$\text{slope} = \frac{k_1 k_2\,[CO] + k_{-1}k_{-2}\,[n\text{-}Bu_3P]}{k_{-1}\,[n\text{-}Bu_3P] + k_2\,[CO]} = k\ \text{obsd.}$$

Due to the complicated form of this rate expression, no simple graphical method yields the kinetic rate constants. Therefore, alternative procedures were used. One method of obtaining data is to look separately at the reverse reaction,

$$RuTPP(CO)(n\text{-}Bu_3P) + n\text{-}Bu_3P \longrightarrow RuTPP(n\text{-}Bu_3P)_2 + CO.$$

After adding one atmosphere of CO to a degassed solution of $RuTPP(n\text{-}Bu_3P)_2$ and allowing the reaction to go to completion, a large excess of phosphine

was added under the CO atmosphere, pushing the reaction in equation 1 completely to the left. Under these conditions, k_1 is negligible, and rate is given by

$$\text{rate} = \frac{k_{-1}k_{-2}\,[\text{n-Bu}_3\text{P}][\text{RuTPP(CO)(n-Bu}_3\text{P)}]}{k_2[\text{CO}] + k_{-1}\,[\text{n-Bu}_3\text{P}]}$$

which may be expressed

$$\text{rate} = k\ \text{obsd}\ [\text{RuTPP(CO)(n-Bu}_3\text{P)}].$$

This can be arranged to give

$$k\ \text{obsd}^{-1} = k_{-2}^{-1} + k_2[\text{CO}]/k_{-1}k_{-2}[\text{n-Bu}_3\text{P}]$$

A plot of k obsd^{-1} versus [CO]/[L] should give a straight line of slope = $k_2/k_{-1}k_{-2}$ and intercept k_{-2}^{-1}, Figure III.6. Because the forward reaction does not go to completion at less than one atmosphere of CO, k_1 cannot be determined directly. However, knowing K, k_{-2}, and k_2/k_{-1}, k_1 can be calculated (Table III.2). The k obsd values calculated from these constants agree with k obsd found experimentally, see Table III.3.

Table III.2. Rate Constants for the Reaction of $\text{RuTPP(n-Bu}_3\text{P)}_2$ and CO at 26°C

$k_1 sec^{-1}$	k_2/k_{-1}	$k_{-2} sec^{-1}$
1.316×10^{-3}	3.366	8.94×10^{-2}

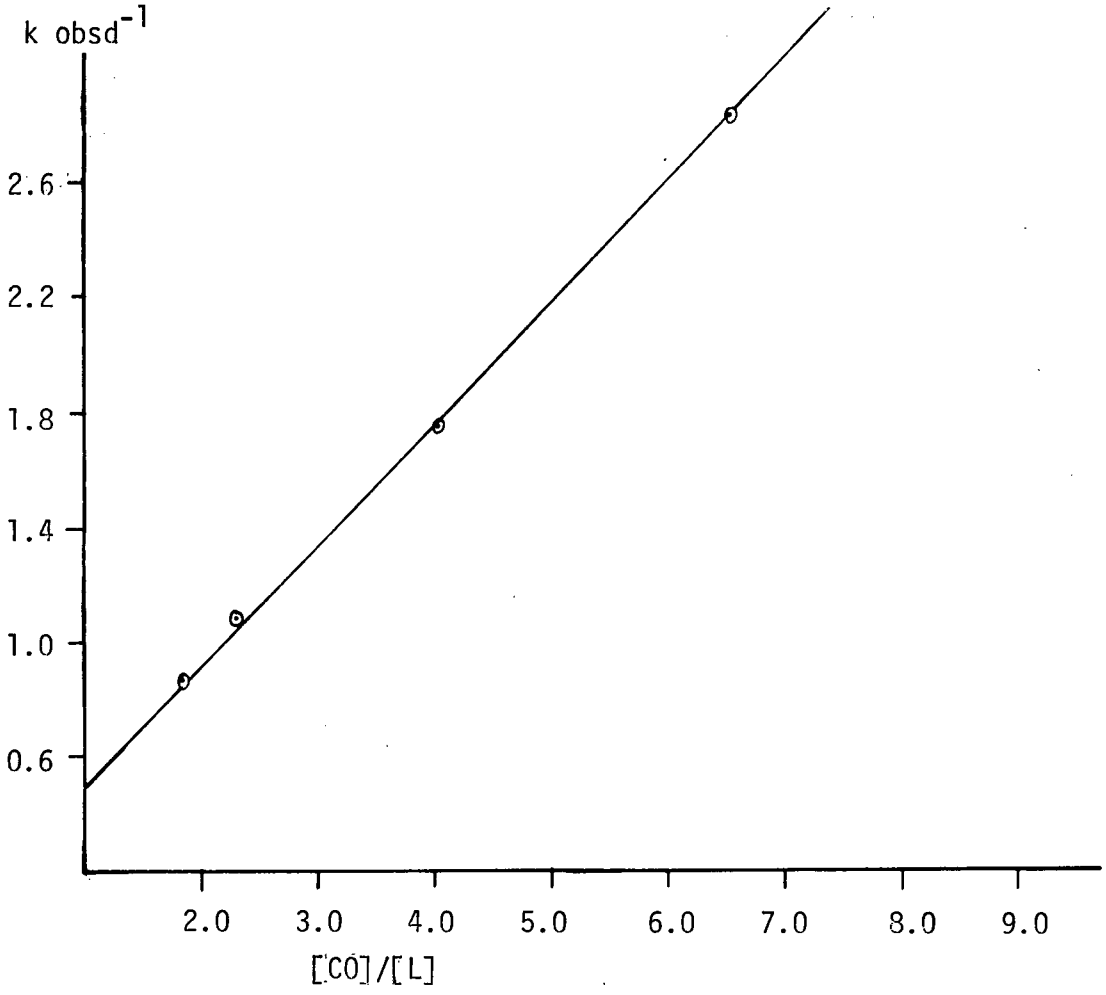

Figure III.6. A Plot of k obsd^{-1} Versus [CO]/[L] for the Reaction of RuTPP(CO)(n-Bu_3P) and n-Bu_3P at 26°C

Table III.3. Reaction of RuTPP(n-$Bu_3P)_2$ with CO in Toluene at 26°C

$[n\text{-}Bu_3P]\times10^4$ moles/litre	CO pressure atm	k obsd x 10^{3a} sec^{-1}	k obsd x 10^{3b} sec^{-1}
1.67	0.966	1.67	2.07
1.98	0.966	1.97	2.21
2.38	0.966	2.08	2.39
3.38	0.966	2.19	2.83
3.90	0.966	2.55	3.06

[a]Found experimentally.
[b]Calculated.

3.3 Discussion

From the data in Table III.2, it is apparent that the six-coordinate bis-phosphine complex of RuTPP(n-$Bu_3P)_2$ loses a phosphine ligand (k_1) ca. 70 times slower than the mixed carbonyl-phosphine species gives up to a CO molecule, (k_{-2}), and this is the major factor governing the equilibrium constant, ($K = k_1k_2/k_{-1}k_{-2}$). The k_{-1}/k_2 value shows that the five-coordinate intermediate has a slight kinetic preference for CO binding over n-Bu_3P. The approximately fifteen-fold difference in the equilibrium constants for the analogous phosphine complexes, RuOEP(n-$Bu_3P)_2$ and RuTPP(n-$Bu_3P)_2$, Table III.4, is reflected in the higher value of k_{-1}/k_2 found in the TPP system. A possible rationale for this may be increased steric hindrance in the TPP system, the phenyl group (at right angles to the porphyrin plane) assisting the removal of the bulky tri-n-butylphosphine group. Steric influences on the binding of CO would be small within the two porphyrin systems.

Table III.4. Kinetic and Equilibrium Data for the Reactions of Fe and Ru Porphyrin Complexes with CO in Toluene

COMPLEX	k_1	k_{-1}/k_2	k_{-2}	K	TEMP.°C
$RuOEP(CH_3CN)_2$[a]	2.41×10^{-3}	0.176	3.4×10^{-7}	4.0×10^{4}	30
$RuOEP(n\text{-}Bu_3P)_2$[a]	2.11×10^{-3}	0.061	5.35×10^{-2}	0.677	31
$RuTPP(n\text{-}Bu_3P)_2$[b]	1.32×10^{-3}	0.273	8.93×10^{-2}	0.054	26
$FeOMBP(pip)_2$[c]	1020	1.7	0.25	2340	23
$FeOMBP(py)_2$[c]	490	26	0.09	209	23
$FePpIX(pip)_2$[c]	20	0.002	0.06	23,000	23
$FeTPP(pip)_2$[c]	11	0.002	0.52	150,000	23
$FePc(pip)_2$[c]	0.5	3.33	0.13	0.85	23

[a] S. Walker, M.Sc. Thesis, University of British Columbia.
[b] This work.
[c] B.R. James, K.J. Reimer and C.T. Wong, J. Am. Chem. Soc. 99, 4815 (1977).

Electronic factors could also play a role as there is a difference in the two porphyrin basicities, see pK_3 in Table III.5. pK_3 refers to the addition of a proton to the neutral porphyrin

$$pH_2 + H^+ \longrightarrow pH_3^+ \quad (pK_3 = pH - \log \frac{[pH_2]}{[pH_3^+]})$$

and is used as a measure of porphyrin basicity. This decreased basicity of TPP leads to a greater affinity for donor ligands and results in stronger metal-porphyrin bonding.[48] This trend has been observed in the study of amine ligand binding to cobalt porphyrin complexes where a decrease in porphyrin basicity correlated with an increase in log K_L, Table III.5.[49] The equilibrium studied was the formation of the 1:1 adducts and K_L refers to the equilibrium constant for that reaction when L = py.

$$L + CoP \rightleftharpoons LCoP$$

equation III.5

The decreased basicity of TPP may also be correlated with the equilibrium constant, K for the carbonylation (equation III.1) and thus to the k_{-1}/k_2 value; this results in a larger k_{-1}/k_2 value, where n-Bu_3P, a better σ donor is favoured over CO, thus increasing k_{-1}.[49] In the analogous OEP complex the increasing basicity results in a smaller value of k_{-1}/k_2.

Table III.5. Log K_L Values for Ligand Binding to a Series of Co Porphyrins

PORPHYRIN	pK_3	log K_L
OEP	6.0	2.85
MpIXDME	5.8	3.25
PpIXDME	4.8	3.78
TPP	3.0	2.92

There is very little difference in the CO 'off' rates for the two bis-phosphine systems, which implies that the dominant factor in k_{-2} is the trans effect of the tri-n-butylphosphine ligand. Comparison of k_{-2} values for the phosphine and acetonitrile systems, shows a difference of the order of 10^5. The high trans effect of tri-n-butylphosphine, being a good π-acid, labilizes CO much more than acetonitrile, which is a poorer π-acceptor.[50]

A hypothesis has been advanced attempting to relate kinetic data, in particular k_{-1}/k_2, to the structure of the five-coordinate intermediate in the reaction mechanism outlined in equation III.2.[51] Data on

$Fe(porp)(amine)_2$ and $FePc(amine)_2$ systems are given in Table III.4, together with those of $Ru(porp)L_2$ systems. The five-coordinate intermediate of the PpIX and TPP systems was considered to have a structure similar to that of A, with the Fe atom out of the porphyrin plane and high spin.[51] Larger values of k_{-1}/k_2, such as those for OMBP and Pc, are thought to be consistent with an intermediate which is low or intermediate spin and has a structure comparable to B. The value of k_{-1}/k_2 obtained for $RuTPP(n\text{-}Bu_3P)_2$ is more comparable to those of the iron OMBP and Pc systems, rather than the TPP system, implying that the intermediate state resembles B more than A, Figure III.7. Comparing the data for the Fe and RuTPP systems, there is a dramatic difference in the values of k_{-1}/k_2, which suggests that the structure of the postulated intermediate is affected by the change in metal. The numbers suggest that the $Fe(porp)(n\text{-}Bu_3P)_2$ geometry would be closer to A, while that of

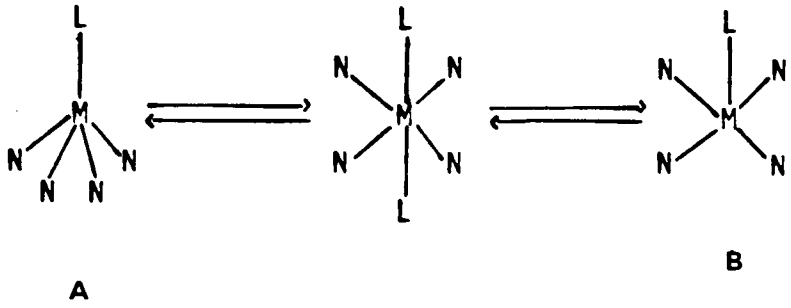

Figure III.7. Possible Structures for the Five-coordinate Intermediate

the ruthenium analogue is closer to B. This effect may be due to the superior π-backbonding ability of Ru(II) compared to Fe(II), tending to keep the metal in the plane of the porphyrin.[52] Of the Fe sub-group, six-coordinate metalloporphyrins, only Fe(II) complexes show high spin states, which is explained by the fact that the energy splitting between the d_{xy}, d_{xz}, d_{yz}, and $d_{x^2-y^2}$, d_{z^2} increases in the order Fe<<Ru<Os.[52]

A recent study on the axial ligand substitution reactions of $Ru(II)PcL_2$ indicates that these reactions again occur via a simple dissociative mechanism.[53]

$$(T)RuPc(L) \underset{+L}{\overset{-L}{\rightleftharpoons}} (T)RuPc + L$$

$$(T)RuPc + X \underset{-X}{\overset{+X}{\rightleftharpoons}} (T)RuPc(X)$$

T = trans group, X = nucleophile, L = leaving group.

The same mechanism holds for $FePcL_2$ systems,[54] and the k_{-1}/k_2 ratios are similar for both Fe and Ru systems. The large difference in k_1 values, Table III.6, shows that $FePcL_2$ systems are more labile than $RuPcL_2$ systems, thought to result from greater (axial) π-backbonding ability of Ru(II). The fact that the k_{-1}/k_2 ratios are similar for ruthenium and iron phthalocyanine systems, whereas fairly large differences exist within analogous porphyrin systems,may be explained by the greater rigidity of the phthalocyanine ligand which tends to keep the Fe more in the plane, such that B represents more the geometry of both

Table III.6. Comparison of Axial Ligand Labilities of Iron and Ruthenium Phthalocyanine Adducts[53]

Trans Group	Leaving Group	$k_1(Fe)/k_1(Ru)$
$P(OBu)_3$	$P(OBu)_3$	20,000
$P(OBu)_3$	MeIm	890
$P(OBu)_3$	py	260
$P(Bu)_3$	$P(OBu)_3$	100,000

k_1 (Fe) at 21°C in acetone.
k_1 (Ru) at 25°C in acetone.

the Fe and Ru five-coordinate intermediates.[55] Thus all three ruthenium porphyrins and possibly ruthenium phthalocyanine systems have five-coordinate intermediates whose structures are similar and are thought to resemble that of B in Figure III.7, with the Ru in the porphyrin plane.

It was hoped that the study of the $RuTPP(n\text{-}Bu_3P)_2$ reaction with CO might give some insight into the mechanism of the catalytic aldehyde decarbonylation reaction, or at least the initiation step, which appears to involve pre-treatment with CO. The relatively high value of k_{-2} indicates that the CO of the monocarbonyl is quite labile as is also suggested by ν(CO) for this complex, see Table I.1. The relatively low K value indicates that the equilibrium (equation III.1) lies to the left when small amounts of phosphine are present, even down to 10^{-5}M. The dramatic effect of tri-n-butylphosphine on the position of the equilibrium implies that the relative concentrations of tri-n-butylphosphine and aldehyde are likely to be critical in the catalytic decarbonylation sequence.

CHAPTER 4

THE CATALYTIC DECARBONYLATION OF ALDEHYDES

4.1 The Use of $RuOEP(CH_3CN)_2$ to Decarbonylate Aldehydes

The title complex was originally selected as a decarbonylation agent because of its rapid and clean reaction with CO in toluene solution,[41] and also because the monocarbonyl thus formed, $RuOEP(CO)(CH_3CN)$ can be conveniently decarbonylated by photolysis in the presence of excess acetonitrile.[42] It was anticipated that the reaction with aldehyde could be made catalytic using visible light, as in equation IV.1.

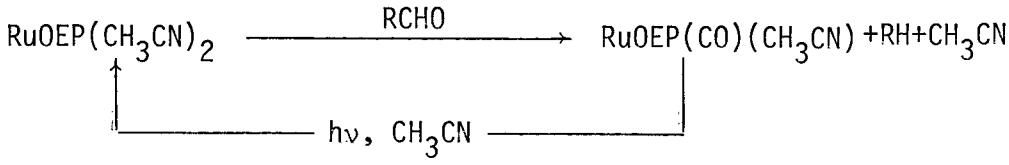

equation IV.1

Benzene was chosen as solvent because of the ready solubility of the OEP complexes in it. Furthermore, the benzene was stable under the conditions of the experiment.

A simple non-catalytic reaction at room temperature was carried out initially using a $1x10^{-4}M$ solution of $RuOEP(CH_3CN)_2$ in degassed benzene containing $10^{-2}M$ phenylacetaldehyde. A rapid (2-5 min) colour change from the characteristic purple of $RuOEP(CH_3CN)_2$ to the orange coloured carbonyl complex, $RuOEP(CO)(CH_3N)$ indicated that decarbonylation had occurred. The spectral changes for the reaction are shown in in Figure IV.1, showing $RuOEP(CH_3CN)_2$ with bands at 527nm ($\log \varepsilon = 4.23$) and 496nm ($\log \varepsilon = 4.02$), shifted to 549nm ($\log \varepsilon = 4.35$) and 518nm ($\log \varepsilon = 4.12$), characteristic of $RuOEP(CO)(CH_3CN)$. The intense Soret

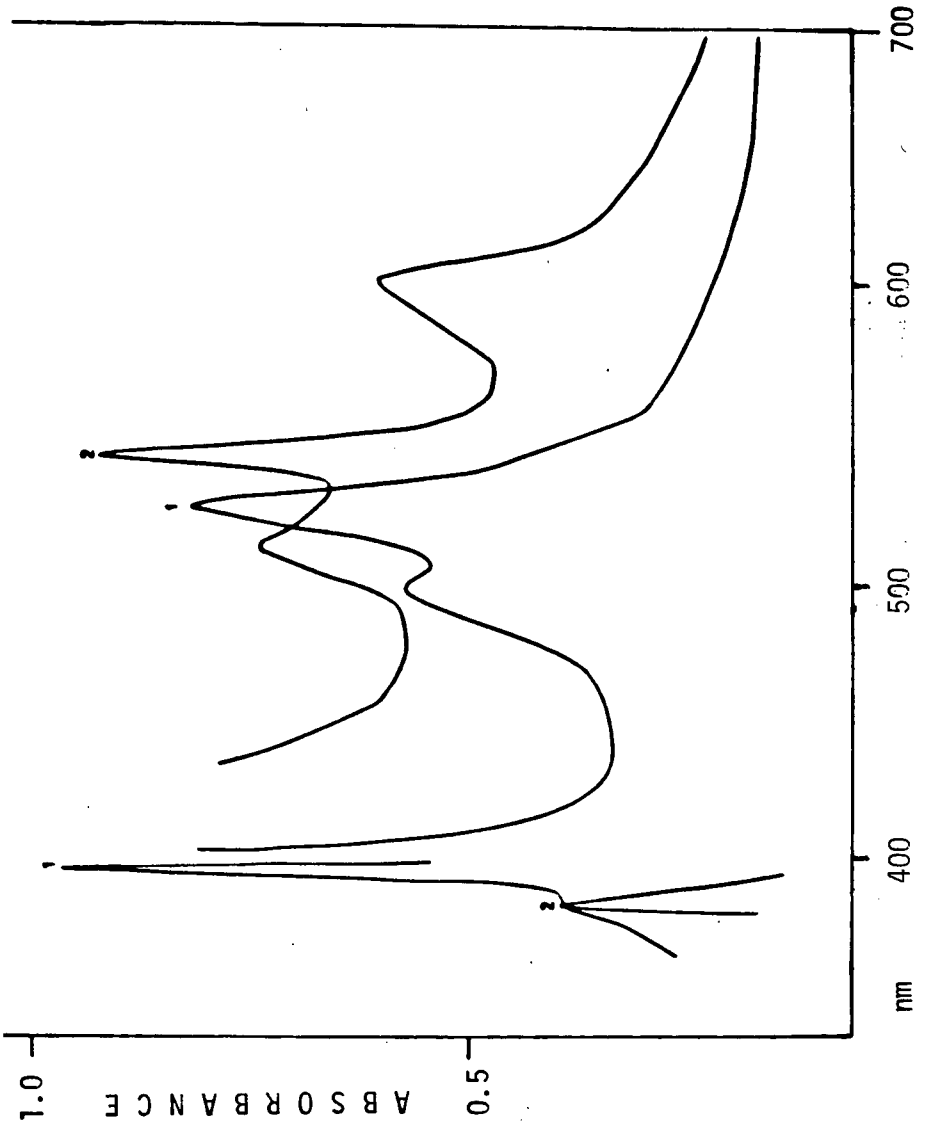

Figure IV.1. The Reaction of $RuOEP(CH_3CN)_2$ with Phenylacetaldehyde at Room Temperature in Benzene. (1) $RuOEP(CH_3CN)_2$, (2) $RuOEP(CO)(CH_3CN)$

band at 405nm (log ε = 5.34) correspondingly shifts to 395nm (log ε = 5.25). An impurity band at ca. 610nm measured in the final spectrum results during addition of aldehyde and is likely due to some oxidation of $RuOEP(CH_3CN)_2$ by impurities in the aldehyde, by comparison with spectral data obtained for air oxidation of this complex.

As excess acetonitrile is thought to be necessary for regenerating the bis-acetonitrile species, the same reaction was carried out in the presence of a three-fold excess of acetonitrile. However, under these conditions no decarbonylation of the aldehyde took place, according to reaction IV.1, over a period of several days.

During the photo-induced decarbonylation of $RuOEP(CO)(CH_3CN)$, a five-coordinate intermediate is probably formed, which then rapidly adds a CH_3CN ligand. Solutions of $RuOEP(CO)(CH_3CN)$ in benzene, with excess phenylacetaldehyde and a ten-fold excess of acetontrile, were irradiated using visible light in the hope that any such five-coordinate intermediate would be capable of abstracting CO, even in the presence of excess acetonitrile. However, no toluene was formed, and no spectral changes were observed. The length of time of photolysis, and concentrations of both aldehyde and acetonitrile (including no added acetonitrile) were varied, but with no success.

The initial rate of the thermal CO abstraction by $RuOEP(CH_3CN)_2$ was quite rapid, and attempts were made to obtain rate constants for the reaction by spectrophotometry. However, the dilute solutions (10^{-5}M in Ru, 10^{-3}M in aldehyde) required for this experiment were easily 'oxidized' by trace impurities in the aldehyde, and no data relevant to the decarbonylation were obtained; the noted isosbestic systems are thought to refer to the oxidation process (Figure IV.2).

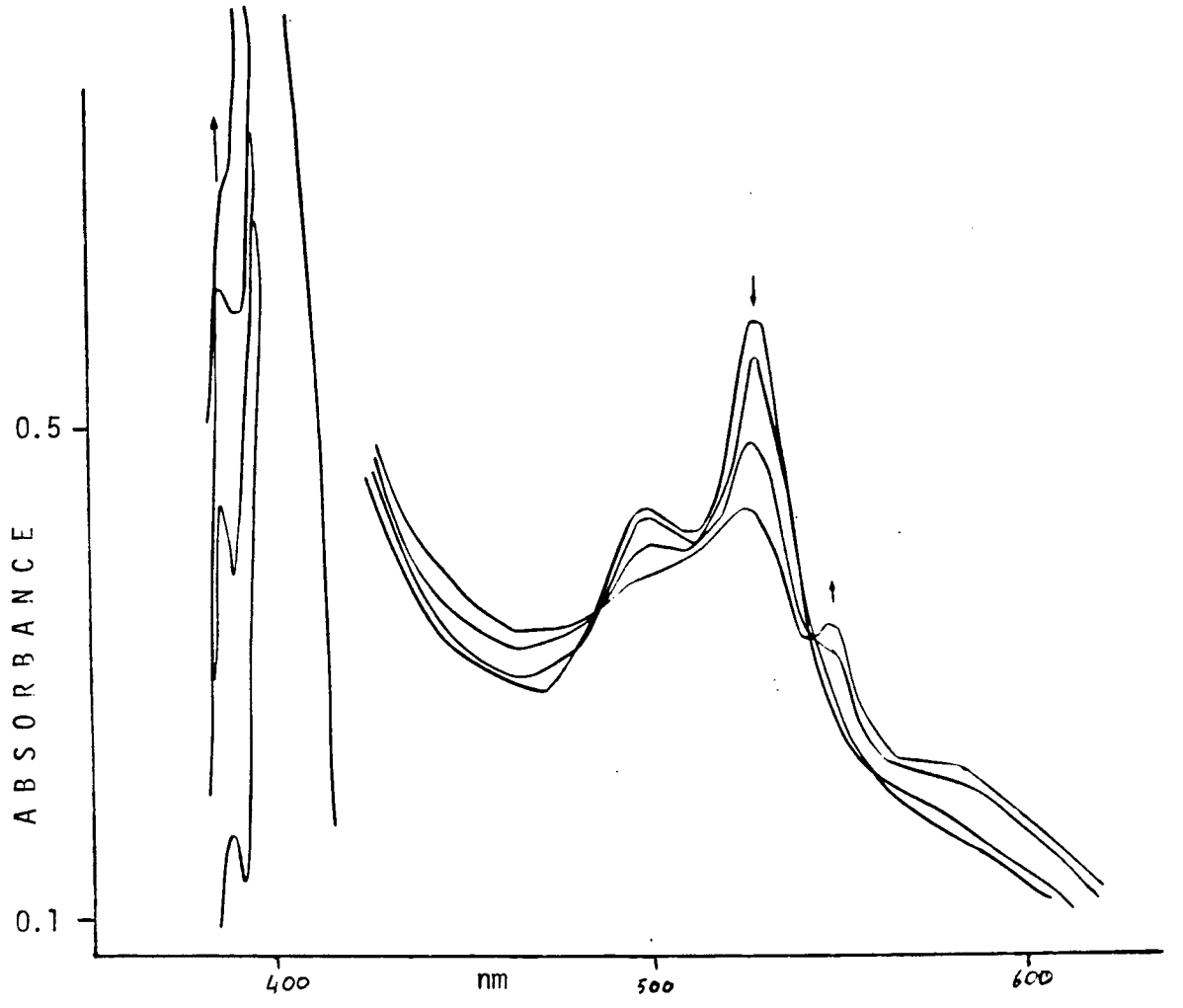

Figure IV.2. The Reaction of $RuOEP(CH_3CN)_2$ with Phenylacetaldehyde at 26°C in Benzene

Other bis species such as $RuOEP(py)_2$, $RuOEP(THF)_2$ were generated in situ, by photolysing the carbonyl in the appropriate solvent, and reacted with phenylacetaldehyde. However, no decarbonylation occurred in the presence of excess axial ligand.

4.2 Discussion

The proposed reaction scheme, equation IV.1, reveals two main problems. Firstly, the reaction

$$RuOEP(CH_3CN)_2 + RCHO \longrightarrow RuOEP(CO)(CH_3CN) + CH_3CN + RH$$

does not proceed in the presence of excess acetonitrile and secondly, successful regeneration of the catalyst from photolysis of $RuOEP(CO)(CH_3CN)$ plus 1 equivalent of acetonitrile does not occur. Since the carbonyl is photo-labile, its displacement by light would not be expected to depend on the amount of excess acetonitrile present. This is shown to be the case in a separate experiment which demonstrated that the reaction,

$$RuOEP(CO)(CH_3CN) \xrightarrow{CH_3CN} RuOEP(CH_3CN)_2 + CO$$

proceeded with only three equivalents of acetonitrile present. If CO were ejected giving a five-coordinate intermediate, such a species, having a vacant coordination site, would be a better candidate for oxidative addition by aldehyde which is the first step in many decarbonylation reactions.[4-12] However, since the only product of photolysis is $RuOEP(CO)(CH_3CN)$, at any added CH_3CN concentration, it was concluded that light would not remove CO in the presence of excess aldehyde. A reaction in which $RuOEP(CO)(CH_3CN)$ was treated with an excess of acetonitrile over aldehyde did result in the formation of $RuOEP(CH_3CN)_2$. There is no possibility of generation of $RuOEP(CH_3CN)_2$ and subsequent

conversion to $RuOEP(CO)(CH_3CN)$ by abstraction from the aldehyde, i.e. catalysis, as no build-up of toluene is observed.

From the kinetic studies[41] on the carbonylation reaction

$$RuOEP(CH_3CN)_2 + CO \longrightarrow RuOEP(CO)(CH_3CN) + CH_3CN$$

the five-coordinate intermediate prefers to bind CO over CH_3CN kinetically by a factor of 5, and also the mixed ligand species gives up a CO ca. 10^4 times more slowly than the bis species loses CH_3CN. If the reaction, equation IV.1, is presumed to follow the same dissociative mechanism, see Chapter 3, the kinetic data could account for the failure of $RuOEP(CO)(CH_3CN)$ to lose CO in the presence of a source of carbonyl, although these data refer to a thermal system. No mechanistic studies have been performed on the photolytic decarbonylation.

The other problem, forcing $RuOEP(CH_3CN)_2$ to abstract CO in the presence of excess acetonitrile, could be possibly overcome by increasing the concentration of aldehyde relative to acetonitrile. In the analogous reaction with CO an excess of CH_3CN does not prevent the carbonylation reaction from going to completion.[41]

4.3 The Use of $RuTPP(PPh_3)_2$ to Decarbonylate Aldehydes

Several ruthenium porphyrin complexes incorporating various phosphine ligands were synthesized in this laboratory,[44] and these were investigated for use as decarbonylation catalysts. The preparation of $RuTPP(PPh_3)_2$ (8), is described in Chapter 2. During the refluxing procedure the position of the $\nu(CO)$ changed from 1950 cm^{-1} to 1915 cm^{-1}, before complete loss of bands in this region. Complex (8) also is known to dissociate a phosphine ligand rapidly in solution, giving an unsual spectrum, see Figure IV.3. A solution of $RuTPP(PPh_3)_2$,

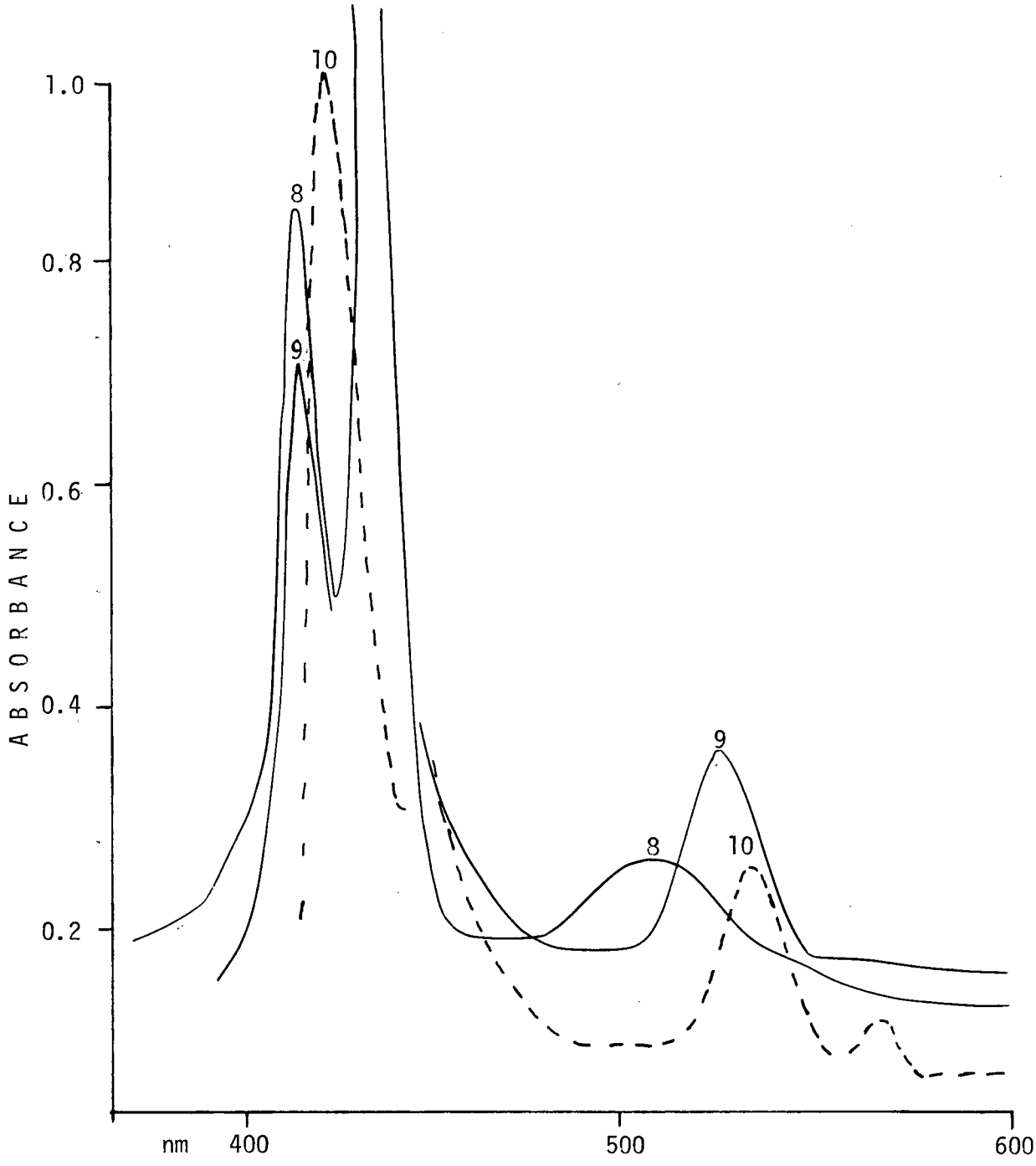

Figure IV.3. $RuTPP(PPh_3)_2$ in CH_2Cl_2 Solution

(8) in CH_2Cl_2 shows absorptions at 412nm, 435nm, and 510nm. Addition of CO gas gives a distinct colour change and a spectrum (9) with bands at 412, 530, and 565nm, respectively, similar to that of RuTPP(CO)(EtOH) species. On addition of triphenylphosphine to this solution a further species (10) is generated, which is neither (8) nor (9), and which has absorptions at 420, 540 and 575 nm. This spectrum is similar to that obtained for RuTPP(CO)(n-Bu_3P) in the presence or absence of excess phosphine and is attributed to RuTPP(CO)(PPh_3). The spectrum of (9) is typical of a RuTPP(CO)(EtOH) species, or other RuTPP(CO)(S) species where S is a weakly coordinating solvent, such as CH_3CN, or THF.[31] Although it is known from X-ray crystal data that S occupies a coordination site in the solid state,[56] it is not clear whether this is true when the complex is in solution. The similarity in the spectra of all of these RuTPP(CO)(S) and the RuTPP(CO)(PPh_3) species suggests that perhaps the sixth axial ligand dissociates in solution, giving a five-coordinate Ru(porp)(CO) species. This implies that in dilute solution and in the absence of excess triphenylphosphine, RuTPP(CO)(PPh_3) dissociates a phosphine according to the following scheme. Addition of excess phosphine to (8) gives the typical bis-phosphine spectrum, with bands at 434 and 515nm.

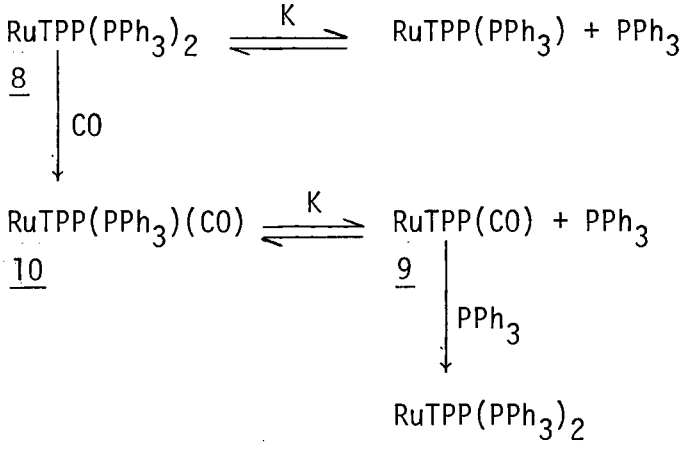

Refluxing or warm solutions of $RuTPP(PPh_3)_2$ in CH_2Cl_2 were employed to decarbonylate phenylacetaldehyde catalytically, but turnover numbers were not very high. Figure IV.4 shows a chromatograph of one such reaction mixture. The turnover numbers were estimated using the internal standard method (by adding a known concentration of a standard compound to a known quantity of the reaction mixture). The response factor of the product being estimated is compared to the response factor of the standard. This ratio of response factors should be constant over the concentration range studied.

Using the rationale discussed in the introduction, the reaction was modified by adding excess tri-n-butylphosphine, which is known to displace CO more readily than triphenylphosphine,[44] and the reaction was carried out in acetonitrile solutions. Typical spectral changes for the catalytic reaction are shown in Figure IV.5. Solutions were initially ca. $5x10^{-5}M$ in Ru, $10^{-2}M$ in aldehyde, and small amounts (5-10 μL) of tri-n-butylphosphine were added. Addition of larger amounts of phosphine gave formation of $RuTPP(n\text{-}Bu_3P)_2$ and no decarbonylation. After addition of phosphine, spectral changes indicated the presence of two species with Soret bands at 435nm (a bis-phosphine) and 416nm, which is likely to be a monocarbonyl complex. The final spectrum obtained, when decarbonylation had ceased, is also shown in Figure IV.5; the main feature is a broad Soret at 410nm. The colour of these inactive solutions was greenish-brown.

The range of turnover numbers obtained for decarbonylation of phenylacetaldehyde under a range of conditions varied considerably, Table IV.1. Several attempts were made to reproduce turnover numbers and reaction rates (Chapter 2). However, the reaction was found to be generally irreproducible, sometimes not showing any catalytic activity

Table IV.1. The Decarbonylation of Aldehydes Using a $RuTPP(PPh_3)_2/n\text{-}Bu_3P$ System[30(b)]

Substrate	Major Product (%)	Conversion (time in hour)	Turn-over (first hour)
C_6H_5CHO	Benzene (100)	10(5)	10
$C_6H_5CH{=}CHCHO$(trans)	Styrene (100)	20(10)	20
$C_6H_5CH_2CHO$	Toluene (95)	30(1), 90(4)	10^3 – 50
p-CN-C_6H_4CHO	Benzonitrile (100)	15(12)	20
n-$C_6H_{13}CHO$	n-C_6H_{14} (65)	10(1)	10^2
2-Ethylbutanal	n-C_5H_{12} (85)	30(1)	10^3
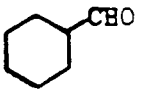	 (60); 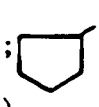 (35) n-C_6H_{14} (5)	30(1), 50(18), 90(50)	2×10^2
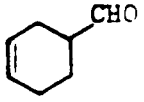	 (70);  (30)	10(1), 20(12)	10^2

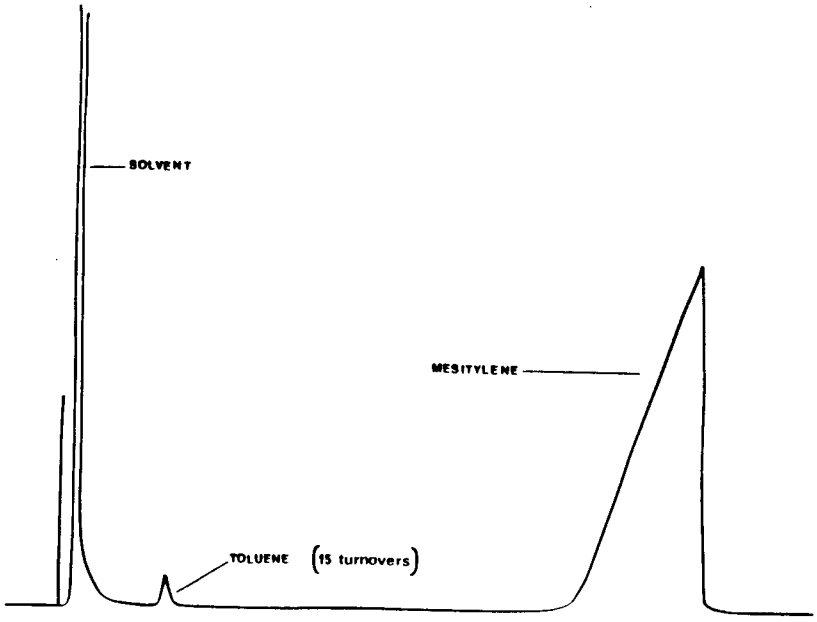

Figure IV.4. The GLC Trace of the Products of the Reaction of $RuTPP(PPh_3)_2$ with Phenylacetaldehyde

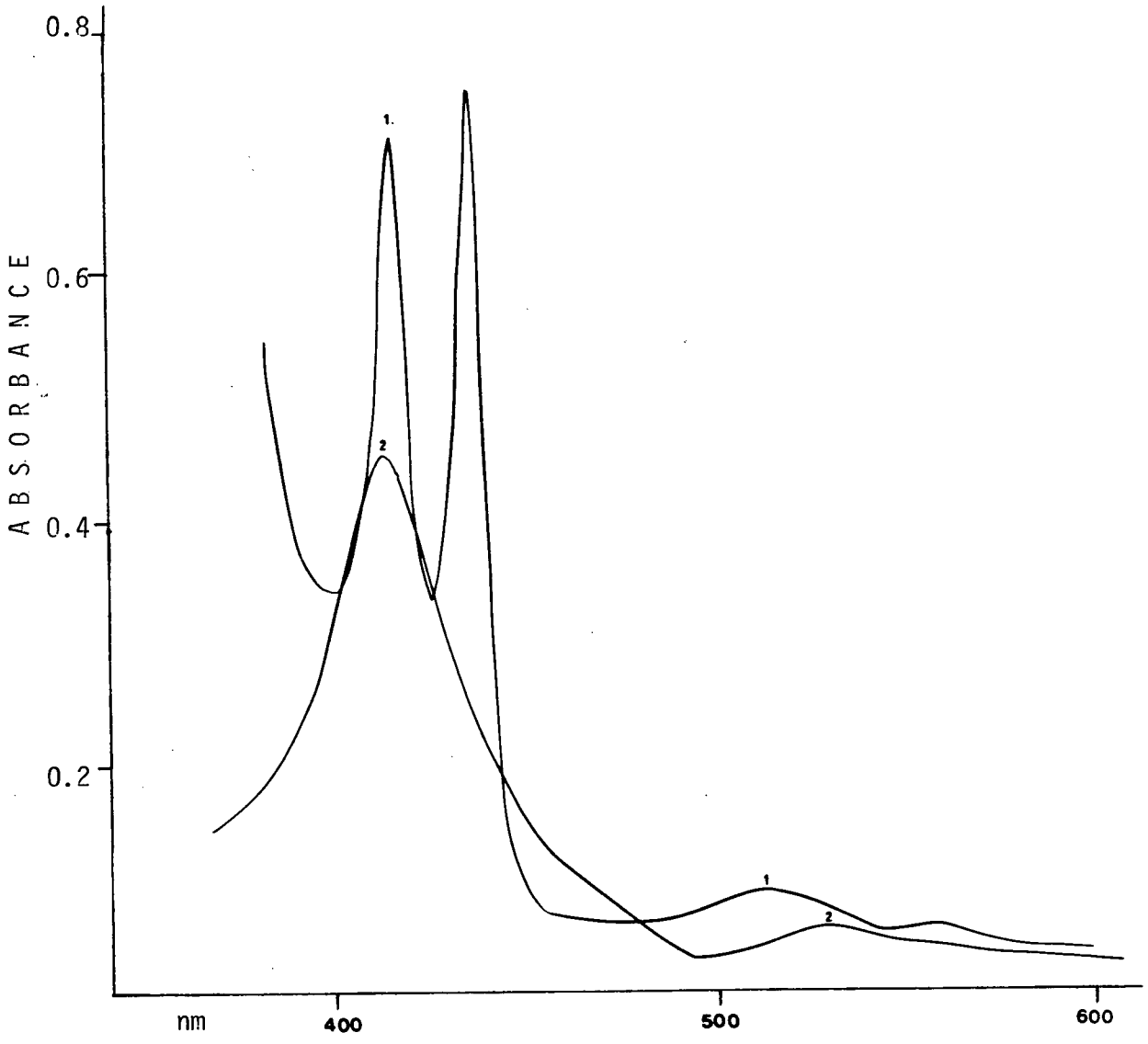

Figure IV.5. Spectral Changes for the Catalytic Decarbonylation of Phenylacetaldehyde Using $RuTPP(PPh_3)_2$/n-Bu_3P as Catalyst. (1) Reaction Mixture After 15 Min. (2) Final Spectrum

while other times yielding very high turnover numbers. Modifications of the experimental procedure still gave variable turnover numbers in a non-reproducible manner.

The general lack of reproducibility and the composition of some of the decarbonylation products (see Table IV.1) indicated that a radical process might be involved. Experiments with radical inhibitors confirmed this; two different radical inhibitors, hydroquinone and 2,6 di-tert-butyl-p-cresol, were found to inhibit production of toluene from phenylacetaldehyde in the catalytic system. Solutions containing the radical inhibitors (at 10^{-3}M) retained their initial orange-red colour for weeks, no spectral changes and no toluene being detected.

4.3.1 Other Aldehydes

A range of aldehydes was investigated, with a view to probing the mechanism of decarbonylation. No general trend was apparent. Heptanal was decarbonylated but the percentage conversion was quite low; in the case of a longer chain aliphatic aldehyde, dodecanal, no decarbonylation took place over several days. Of the aromatic aldehydes, benzaldehyde proved difficult to decarbonylate. After several unsuccessful attempts, some decarbonylation products were eventually detected by another worker in this laboratory.[57] Two of the substituted benzaldehydes (p-nitro and p-cyano) gave somewhat higher turnover numbers than benzaldehyde, but there was no indication of a relationship between catalytic activity and the substitution pattern of these aldehydes. The decarbonylations seem to be reasonably selective with aromatic aldehydes, yielding the expected product. However, small amounts of other products were obtained when an aliphatic system was decarbonylated, Table IV.1. The decarbonylation of cyclohexanecarboxaldehyde, which was carried out

in benzonitrile, yielded two products which were collected in a cold trap and identified by GC-MS as cyclohexane and methylcyclopentane.

All attempts to isolate the ruthenium end product or any intermediates using conventional chromatographic techniques were unsuccessful.

4.3.2 Further Studies

In addition to the studies described above, various other experiments were carried out in an attempt to elucidate details of the reaction mechanism.[a] These are described here because of their relevance to the discussion of the catalytic reaction.

Cyclic voltammetry was performed on both $RuTPPL_2$ systems (L = tri-n-butylphosphine, triphenylphosphine) and also the $RuTPP(PPh_3)_2/n\text{-}Bu_3P$ catalytic system, and some evidence for Ru(III) intermediates comes from these voltammograms. During decarbonylation of the indane aldehyde, some irreversible waves were seen at -0.1V, and in the corresponding phenylacetaldehyde system, waves at -0.08V and +0.08V were thought to result from Ru(III) species.

Infra-red measurements during decarbonylation of the indane aldehyde revealed a small peak at 2015 cm^{-1}, which could be due to a Ru(III) hydride.[30]

Some e.s.r. studies were also performed, using the very slow catalytic decarbonylation of pyridine-2-aldehyde, and cyclohexen-4-al. Organic free radicals, g = 2.00, were detected in both of these systems. During decarbonylation of phenylacetaldehyde, a low temperature broad signal at g = 2.20 was assigned to a low spin d^5 Ru(III) species, although Ru(III) porphyrin systems do not normally give detectable

---

[a]Work performed by G. Domazetis, P.D.F.

e.s.r. signals.[58] Kinetic studies were hampered by the lack of reproducibility. A first-order dependence on aldehyde was observed, but the rate constants were not reproducible.

4.4 Discussion

The generally accepted mechanism of decarbonylation, involving oxidative addition of aldehyde, CO migration, and reductive elimination, would appear to be unlikely for this system. This mechanism would require coordination numbers greater than six, and also Ru(IV) intermediates, which are unusual, though plausible.[22]

The data so far suggest a radical mechanism, and Ru(III) intermediates. A tentative mechanism is outlined in scheme IV.1. Decarbonylation of the acyl radical is thought to be metal assisted, giving

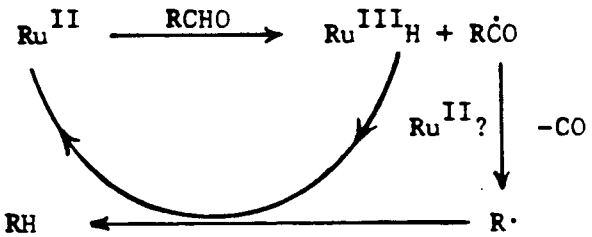

Scheme IV.1. The Mechanism of Decarbonylation Using the $RuTPP(PPh_3)_2/n\text{-}Bu_3P$ System

a Ru(II) carbonyl, which is subsequently decarbonylated by nucleophilic attack by tri-n-butylphosphine. This phosphine can displace coordinated carbonyl, as exemplified by the reaction

$$RuTPP(CO)(n\text{-}Bu_3P) + n\text{-}Bu_3P \underset{}{\overset{K}{\rightleftharpoons}} RuTPP(n\text{-}Bu_3P)_2 + CO$$

This reaction occurs thermally in toluene at 26°C with a K value of 18.5, see Chapter 3.

It was hoped that identification of the species present during catalysis would be accomplished via spectrometry. The spectral changes for the catalytic reaction are shown in Figure IV.5. After addition of aldehyde (or CO) and tri-n-butylphosphine, two bands appear in the Soret region; one at 435-437nm due to a bis-phosphine species, the other usually found between 416 and 418nm, is probably due to a carbonyl adduct. In the visible region a band at 510nm shifts to 530nm with a band at 560nm. The spectral characteristics of this region are very similar to those of $RuTPP(PPh_3)_2$ after addition of CO (see Figure IV.3), although the bis(tri-n-butylphosphine) complex also has absorptions close to these wavelengths, at 527nm and 560nm. There are no absorptions due to the $RuTPP(CO)(n\text{-}Bu_3P)$ species, which has a Soret band at 420nm. From the spectral data it may be concluded that in the active catalyst solutions there are two main species present. One is a bis-phosphine, either a mixed phosphine system, or a bis(tri-n-butylphosphine) system, and the other may be RuTPP(CO)(S), a solvated species.

The final spectrum, obtained when catalysis is complete, usually after 4-24 hours, has a Soret band which appears from 405-415nm with a band at 530nm and a shoulder at 560nm. This spectrum is common to all the decarbonylations, irrespective of the aldehyde, and seems to be that of a RuTPP(CO) species.

4.4.1 The Role of the Phosphine Ligands

From some experiments with $RuTPP(n\text{-}Bu_3P)_2$, which does not appear to catalytically decarbonylate phenylacetaldehyde, it seems that the triphenylphosphine ligand is necessary for the catalytic reaction, either in an initiation step or a propagation step. This role is probably related to the manner in which $RuTPP(PPh_3)_2$ dissociates a

phosphine in solution. The dissociation of phosphine from $RuTPP(PPh_3)_2$ is unusual, as the analogous $RuTPP(n\text{-}Bu_3P)_2$ complex shows no such behaviour. This dissociation may be germane to the catalytic decarbonylation reaction.

4.4.2 The Role of Acetonitrile

As mentioned previously, nitrile solvents have been found to stabilize three coordinate intermediates in decarbonylation reactions,[1] thus preventing dimerization of the active species. The nitrile solvents may have the same type of effect in the present system, i.e. preventing dimerization or aggregation of unsaturated intermediates. However, it is more likely that the formation of solvated species such as RuTPP(phosphine)(CH_3CN), for which there is some spectral evidence, is the primary role of acetonitrile. Benzonitrile appears to have the same effect as acetonitrile and was used in many reactions where volatile products were being collected. The catalytic reaction does occur in absence of nitrile solvents, but yields were not as good in CH_2Cl_2 alone.

There is evidence, then, for the occurrence of Ru(III) intermediates from e.s.r. data and also cyclic voltammetry. If a relatively high concentration of Ru(III) built up, it should be observable in the visible spectrum of the catalyst solution, although small amounts would not be detectable. There is also strong evidence for a radical type mechanism. The fact that the catalytic reaction was totally inhibited by radical inhibitors, for several trials, indicates that free radicals are definitely involved. The other evidence for these comes from e.s.r. where signals due to free radicals were detected in frozen catalyst solutions. Formation of $\dot{R}$ species is also favoured in view of the MS of the decarbonylated cyclohexanealdehyde which revealed the presence

of methylcyclopentane as a product. The rearrangement shown below is plausible, as the 5-hexene-1-yl radical is known to rearrange as shown.[59]

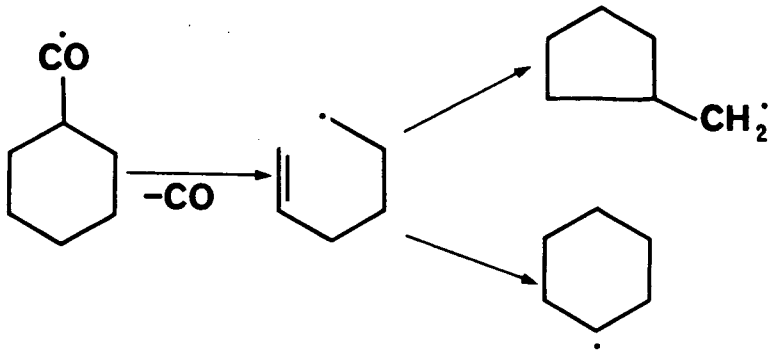

This $\dot{R}$ species could be stabilized by a metal complex, in a cage reaction. This type of mechanism was considered by Walborsky and Allen[60] for the stoichiometric decarbonylation of aldehydes by $RhCl(PPh_3)_3$. The irreproducibility of the reaction and poor kinetic data also support

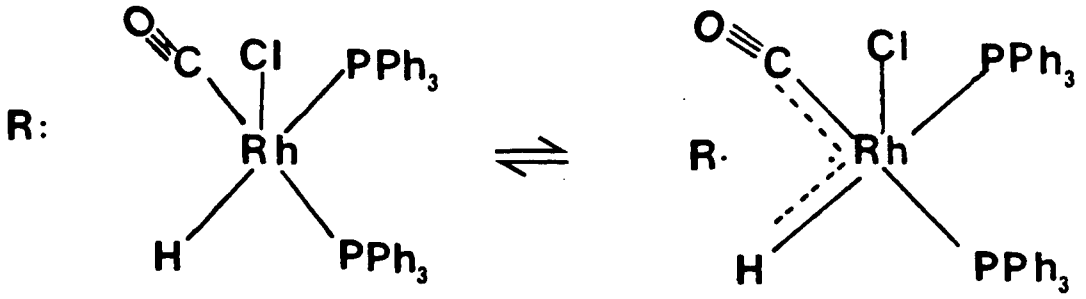

Scheme IV.2. The Decarbonylation of Aldehydes Using $RhCl(PPh_3)_3$

this theory. It is possible that the eventual destruction of the porphyrin ring is also a result of a radical attack on the porphyrin.

CHAPTER 5

THE STOICHIOMETRIC REACTION OF $RuTPP(n\text{-}Bu_3P)_2$ WITH PHENYLACETALDEHYDE

5.1 Kinetics and Spectral Characteristics

This reaction was studied with a view to elucidating the mechanism of the catalytic reaction discussed in Chapter 4, in particular the nature of the initiation step of the reaction, in which the monocarbonyl, $RuTPP(CO)(n\text{-}Bu_3P)$ is thought to be formed.

Dichloromethane was chosen as solvent initially because of the ready solubility of the porphyrin complexes in it, and also to facilitate any detection of toluene. To ensure that only a stoichiometric decarbonylation was taking place, the reaction mixture was tested for toluene by GLC, at the end of the reaction. Toluene was not detected at low concentrations of ruthenium catalyst, and a stoichiometric amount was detected at 10^{-3}M ruthenium.

$$RuTPP(n\text{-}Bu_3P)_2 + RCHO \longrightarrow RuTPP(CO)(n\text{-}Bu_3P) + RH + n\text{-}Bu_3P$$

equation V.1

The reaction was followed spectrophotometrically, and several clean isosbestic points were observed, Figure V.1. The direction of these spectral changes was the same as that observed for the analogous reaction with CO, Chapter 2. At high aldehyde to ruthenium ratios, and in the absence of added excess phosphine, the reaction exhibited pseudo-first-order dependence as shown by plots (Figure III.2) of $\log\left(\frac{A_t - A_\infty}{A_o - A_\infty}\right)$ versus time, where

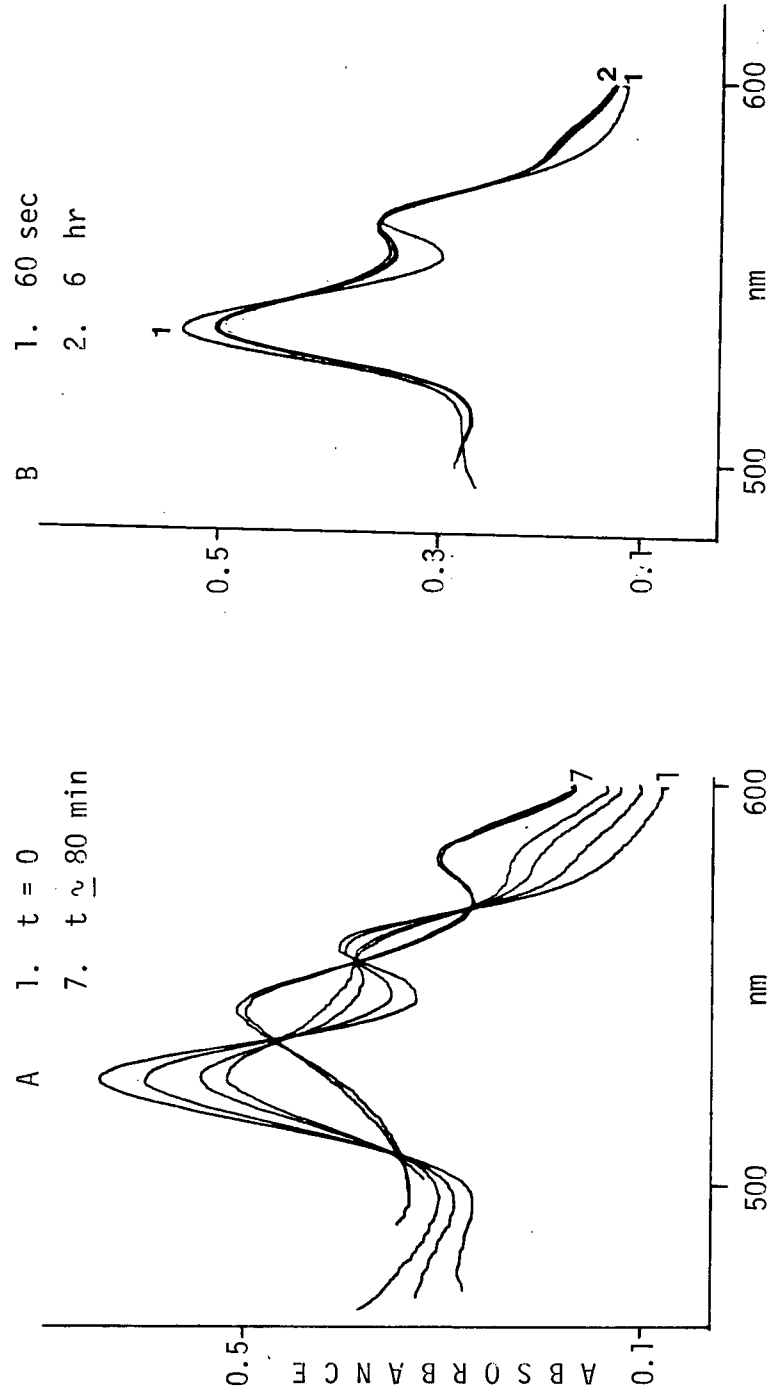

Figure V.I. The Reaction of $RuTPP(n\text{-}Bu_3P)_2$ with Phenylacetaldehyde [3.42×10^{-2}M] in CH_2Cl_2 at 26°C, (A) and in Toluene, (B)

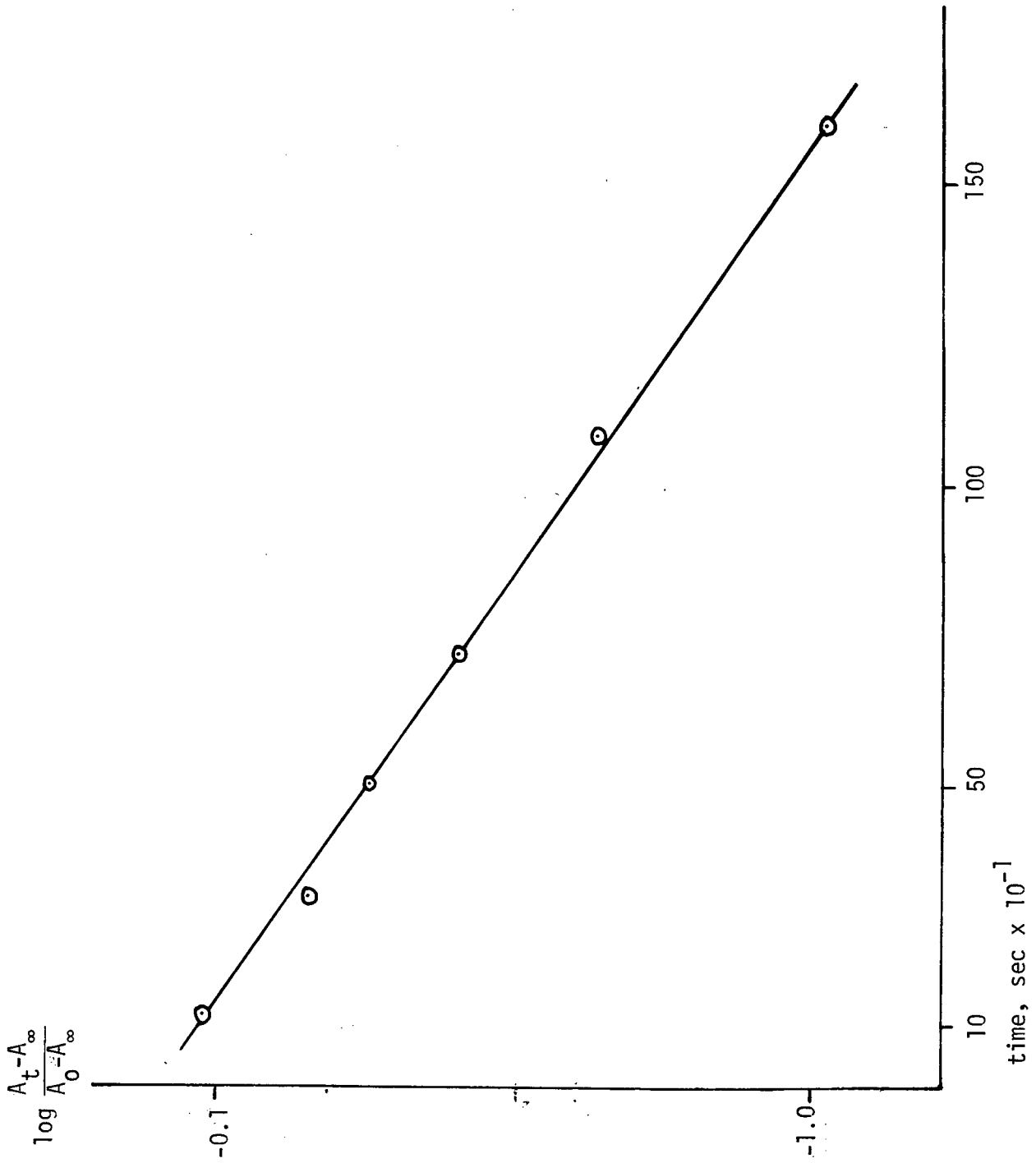

Figure V.2. First Order Plot for Reaction of $RuTPP(n\text{-}Bu_3P)_2$ with 3.42×10^{-2} M Phenylacetaldehyde at 26°C

A_t = absorption at time, t

A_∞ = absorbance of final species

A_0 = absorbance of initial species

In the presence of any added phosphine, even one mole/Ru, the reaction did not proceed and no carbonyl was formed.

Table V.1 shows the various k obsd values obtained for varying concentrations of ruthenium at the same initial concentration of

Table V.1. k obsd Values Obtained for Various Ru(II) Concentrations at 3.42×10^{-2}M Aldehyde

[Ru(II)]x10^5 moles/litre	k obsd x 10^3 sec^{-1}
3.28	1.52[a]
2.69	1.57[a]
3.66	1.21[a]
1.90	1.53[a]
3.33	1.01[a]
3.66	1.21[a]
4.11	0.96[b]
1.90	1.27[b]
2.66	1.73[b]
2.69	1.57[b]
2.58	0.78[c]
1.69	1.16[c]
5.08	1.50[c]

[a]First batch.
[b]Second batch.
[c]Third batch, addition of O_2 after degassing.

aldehyde. The value of k obsd was not independent of the ruthenium concentration (the normal behaviour for first-order dependence on ruthenium) and there was no regular trend in k obsd as a function of the ruthenium concentration. Thus, although each individual run showed good first-order behaviour, the evaluated k obsd values were scattered and non-reproducible. An attempt was made to study the dependence on aldehyde concentration, however, this was complicated by the interference of a secondary reaction, which occurred at the higher aldehyde concentrations, see below. Using the extinction coefficients of the carbonyl complex, more careful analysis revealed that the reaction was not going to completion as originally assumed, but appeared to be going to an equilibrium position. This raised the possibility of the toluene product being involved in an equilibrium such as:

$$RuTPP(n\text{-}Bu_3P)_2 + RCHO \rightleftharpoons RuTPP(CO)(n\text{-}Bu_3P) + Bu_3P + RH$$

equation V.2

which could imply a potentially exciting carbonylation of toluene! Indeed, the reaction when carried out in toluene, Figure V.1, did not proceed to any appreciable extent. However, addition of small amounts of toluene, e.g. 100-fold excess over ruthenium had little effect on the measured k obsd values or the apparent equilibrium position, which argues against an equilibrium involving toluene. An attempt was made to reverse the reaction, equation V.3.

$$RuTPP(CO)(n\text{-}Bu_3P) + Bu_3P \xrightarrow{\text{Toluene}} RuTPP(n\text{-}Bu_3P)_2 + C_6H_5CHO$$

equation V.3

However, no visible absorption bands due to $RuTPP(n\text{-}Bu_3P)_2$ were observed.

The use of higher concentrations of aldehydes usually resulted in a loss of isosbestics and general broadening of the spectrum in the 530nm region, before the 'A_∞' of the decarbonylation reaction could be recorded, Figure V.3. This problem was circumvented by using a Guggenheim analysis of the data for which 'A_∞' does not have to be known.[61] Figure V.4 shows some data obtained for one set of runs but later sets were found to be irreproducible. The secondary reaction appeared to be related to the purity and amount of the aldehyde used. It was initially suspected that this reaction may have been a degradation reaction involving attack on the porphyrin ring. However, addition of excess tri-n-butylphosphine to solutions in which the 'secondary' reaction has taken place regenerated the initial spectrum completely, Figure V.3, indicating that the 'secondary' reaction is not porphyrin breakdown and is probably a reversible oxidation reaction. However, if the reaction solutions were left to stand for more than 1-2 days, only partial regeneration of the bis species was achieved. Some impurity in the aldehyde was thought to be responsible for the 'secondary' reaction, but it was not clear from the data whether the RuTPP(CO)(n-Bu_3P) product, or the RuTPP(n-$Bu_3P)_2$ starting material was being oxidized. Some redox studies were carried out to help resolve this oxidation problem.

5.2 The Bromine Oxidation of RuTPP(n-$Bu_3P)_2$

Bromine oxidation of RuTPP(n-$Bu_3P)_2$ was considered likely to generate Ru(III)TPP(n-$Bu_3P)_2$. Small aliquots of a $1x10^{-2}$M bromine solution in CH_2Cl_2 were therefore added to a $5x10^{-2}$M Ru(II) solution until oxidation was complete, as judged by spectral changes, Figure V.5. There was a loss of intensity at 527nm and 560nm, giving rise to a broad absorption in this region, with a shoulder at 580nm. Absorption at

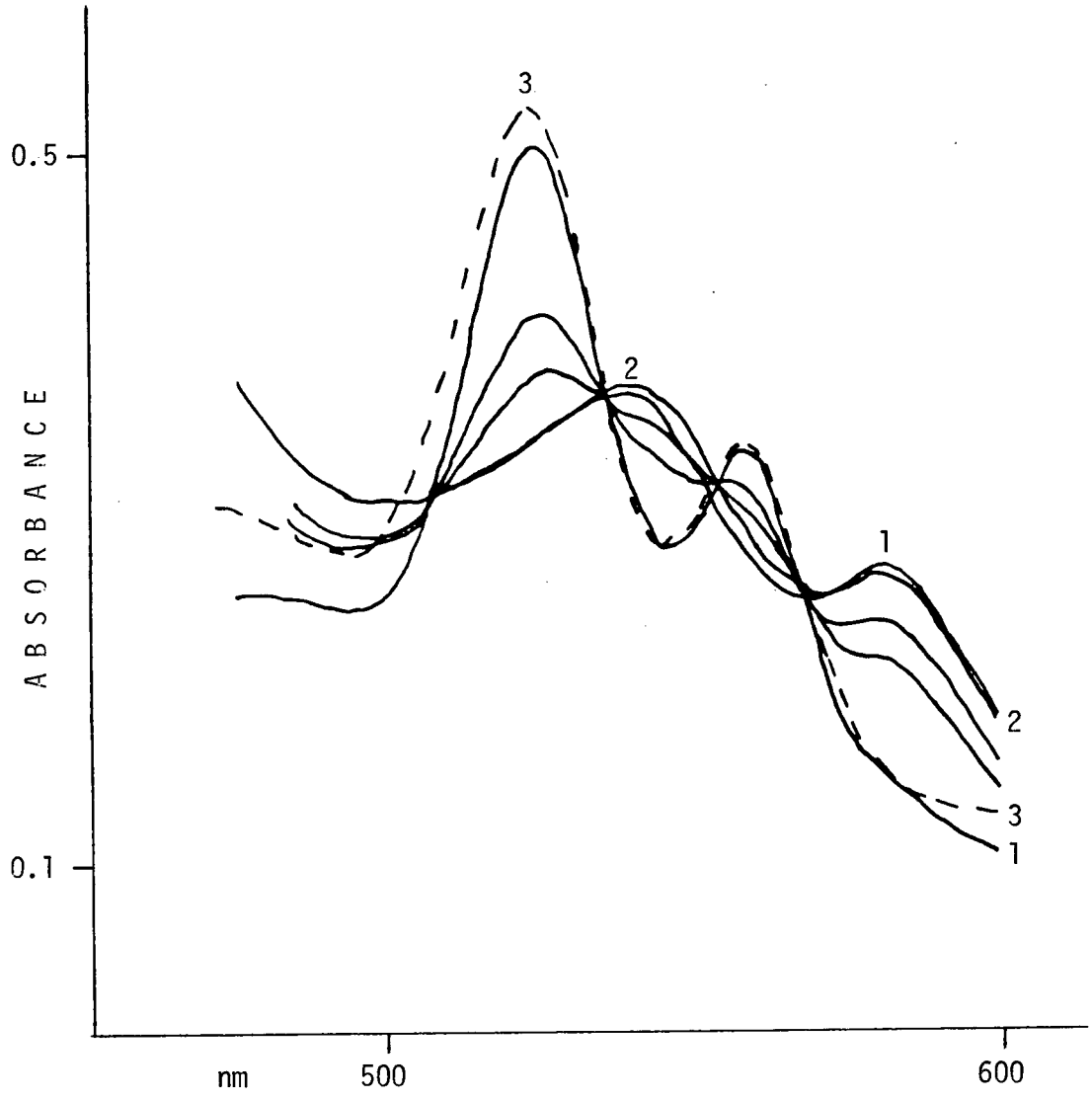

Figure V.3. Reaction of $RuTPP(n\text{-}Bu_3P)_2$ with Phenylacetaldehyde Showing Secondary Reaction (2). (3) is the Spectrum Obtained after Addition of $n\text{-}Bu_3P$ to (2)

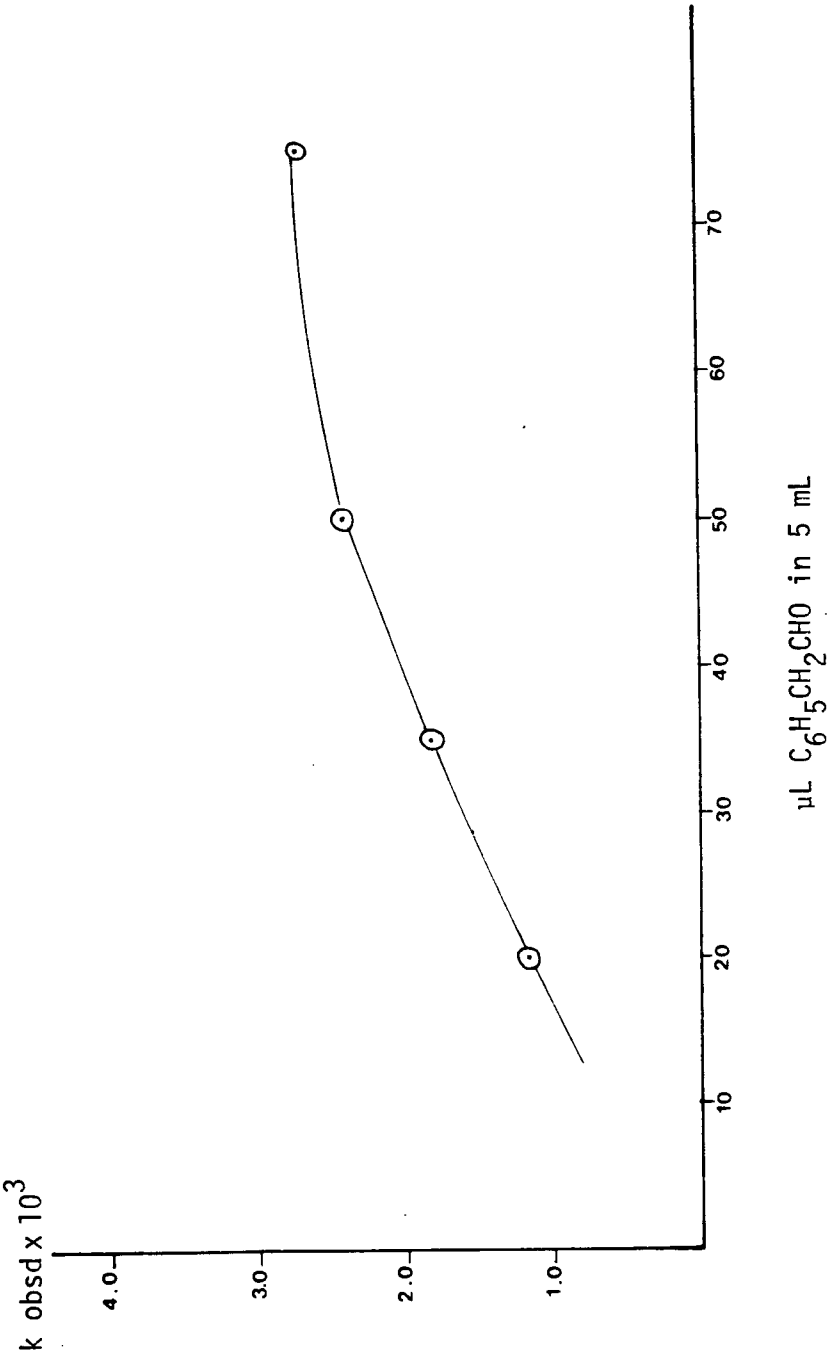

Figure V.4. A Plot of k obsd Versus µL of Phenylacetaldehyde

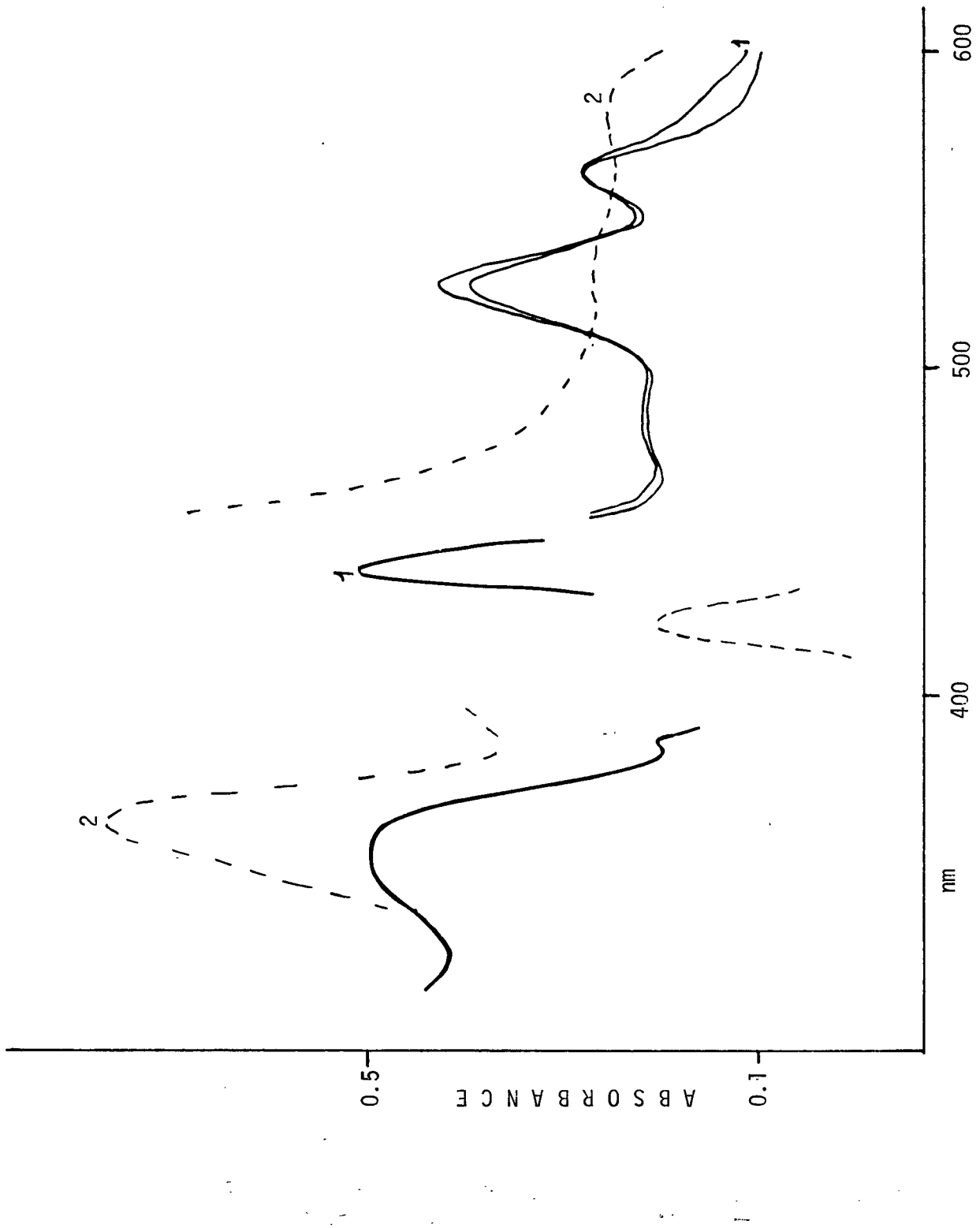

Figure V.5. Spectral Changes for the Bromine Oxidation of $RuTPP(n\text{-}Bu_3P)_2$ in CH_2Cl_2 (1). The Final Spectrum (2)

437nm decreased, and the Soret shifted to 424nm. The increased absorption at 360nm is typical of Ru(III) metalloporphyrin complexes, as are the other spectral changes. The isosbestic points and the general spectral changes for this oxidation reaction are similar to those obtained for the reaction of $RuTPP(n\text{-}Bu_3P)_2$ with phenylacetaldehyde. The colour of the solution after bromine oxidation is olive green and addition of TBAB[62] or tri-n-butylphosphine regenerates the initial spectrum of $RuTPP(n\text{-}Bu_3P)_2$.

5.3 The Bromine Oxidation of $RuTPP(CO)(n\text{-}Bu_3P)$ in CH_2Cl_2

Spectral changes for this reaction are shown in Figure V.6. There is a general decrease and broadening of all the absorptions, giving a less intense Soret at 422nm and a featureless visible region. A broad absorption at ca. 360nm is again indicative of Ru(III) formation. Reduction of this bromine-oxidized solution with TBAB did generate a spectrum similar to that of the carbonyl, but some loss in resolution had occurred. The colour of the oxidized solution again is dark green. The general features of this oxidation imply that it is Ru(II) to Ru(III) oxidation, and not π-cation radical formation by oxidation of the porphyrin ring, see below.

It has been shown that oxidation of Ru(porp)(CO)(L) complexes, where L = amines, always occurs at the porphyrin ring rather than at the metal,[63] although a recent study on the influence of axial ligands on the redox potentials of $RuTPPL_2$ systems claims that oxidation occurs at the metal atom, even when CO is a ligand.[44] It was of interest, then, to do a controlled electrochemical oxidation of $RuTPP(CO)(n\text{-}Bu_3P)$ to see if the product of this type of oxidation might differ from the product of a bromine oxidation.

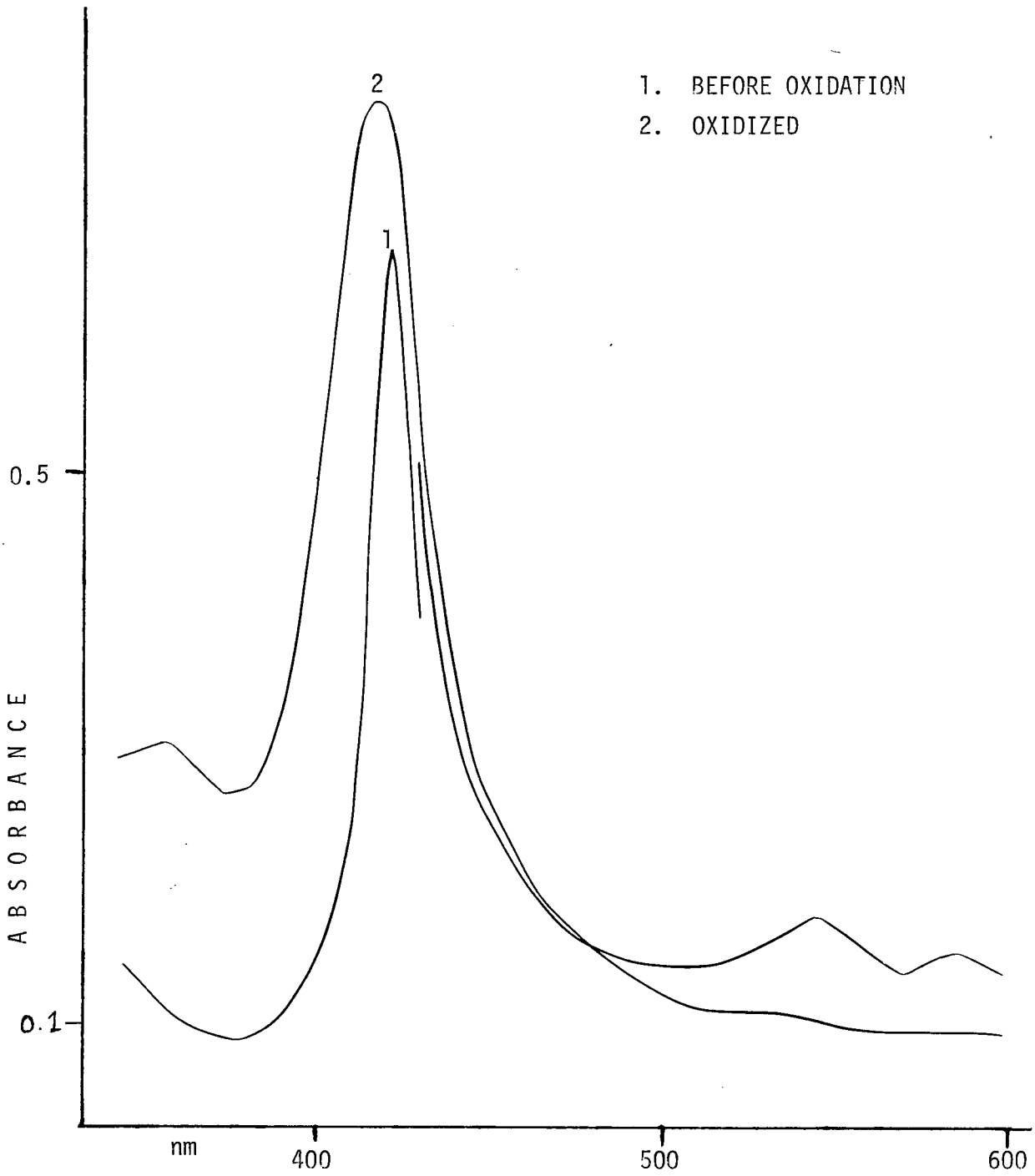

Figure V.6. Spectral Changes for the Bromine Oxidation of $RuTPP(CO)(n\text{-}Bu_3P)$ in CH_2Cl_2

An electrochemical oxidation of the carbonyl complex, from 0.0 to +2.0V, was carried out in a solution of toluene-acetonitrile (1:1) using 0.1M $n\text{-}Bu_4N^+ClO_4^-$ as the supporting electrolyte. A cyclic voltammogram was obtained, Figure V.7, with waves at 0.42V, 0.77V, and 1.0V. The

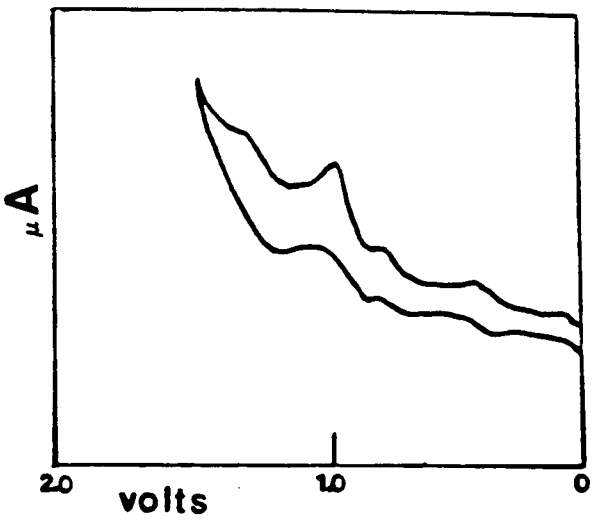

Figure V.7. Cyclic Voltammetry of $RuTPP(CO)(n\text{-}Bu_3P)$ in Toluene-Acetonitrile with 0.1M Electrolyte

main peak, 1.0V is thought to be due to a π-cation radical by comparison with other findings in this laboratory.[64] The other minor peaks are thought to be due to some impurities. The solution was then electrolysed at 1.0V, yielding an olive-green solution, whose spectral characteristics are shown in Figure V.8. The peak at 640nm is typical of cation radical formation.[64] Addition of TBAB to this solution yields an orange-red solution which appeared, from its spectral characteristics, to be a mixture of $RuTPP(CO)(CH_3CN)$ and $RuTPP(n\text{-}Bu_3P)_2$. The broad band at 530nm with a shoulder at 560nm and a Soret at 412nm is typical of RuTPP(CO)S.[31] A second Soret at 437nm indicates the presence of a small amount of $RuTPP(n\text{-}Bu_3P)_2$, the remainder of the spectrum being masked by that of the carbonyl complex. These results imply that during electrochemical

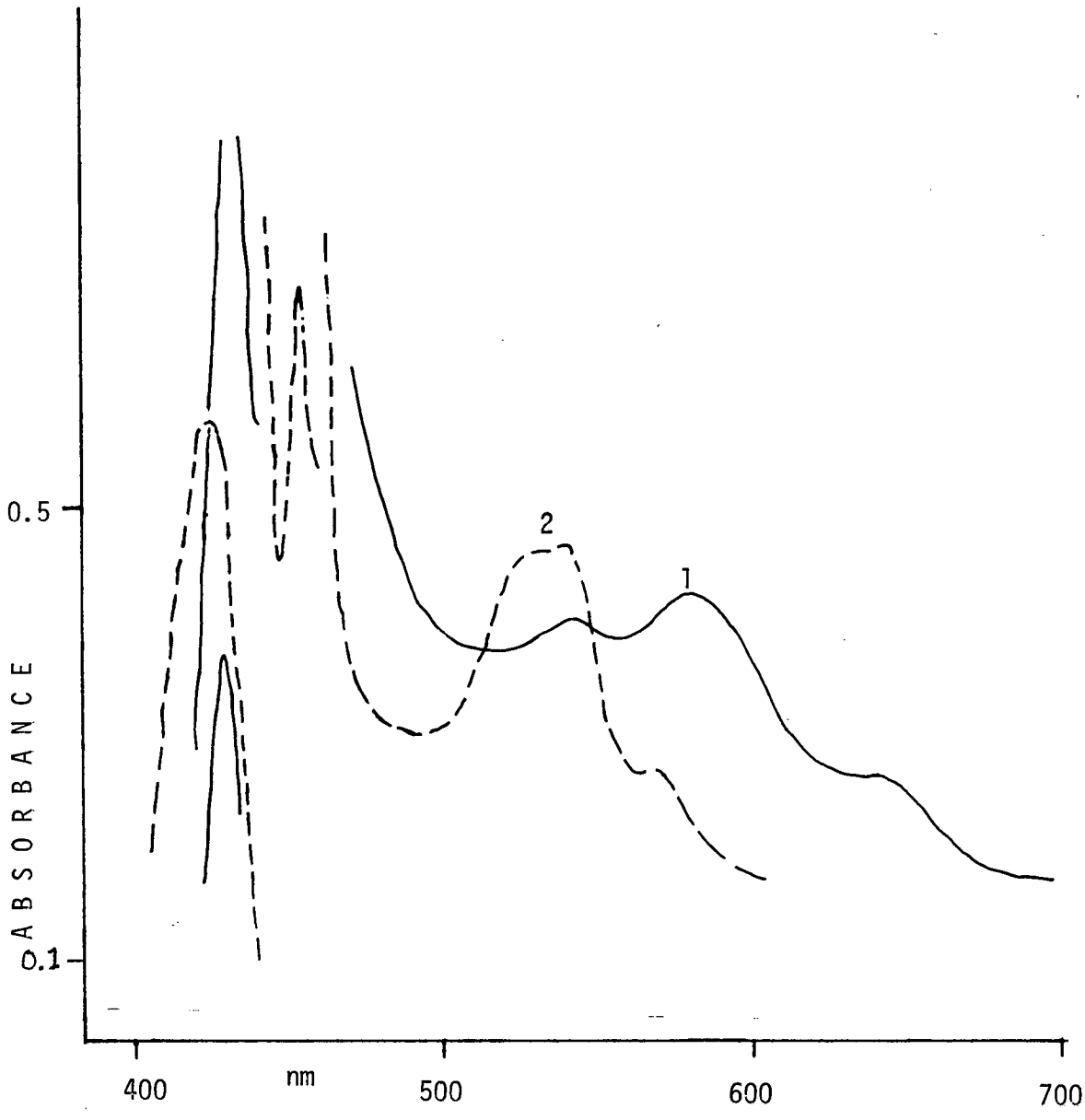

Figure V.8. Product of Electrochemical Oxidation of $RuTPP(CO)(n\text{-}Bu_3P)$ (1). After Reduction with TBAB (2)

oxidation RuTPP(CO)(n-Bu_3P) is converted to $RuTPP^{+\cdot}$(CO)(n-Bu_3P) which possibly loses a phosphine ligand. The presence of this excess phosphine in solution may be the reason for the formation of a small amount of the bis species after reduction. A solution of the cation radical, sealed under argon, was found to revert to the reduced RuTPP(CO)S after a few hours. This behaviour is typical of π-cation radicals in solution.

5.4 Effect of Oxygen on the Stoichiometric Decarbonylation Reaction

The rate of decarbonylation varied irreproducibly from one experiment to another and this variation was not related to the concentration of the ruthenium starting material, Table V.1. In an attempt to make the reaction more reproducible the solutions were degassed by three freeze-thaw cycles prior to addition of aldehyde. In some cases the aldehyde was added to the solvent and degassed prior to addition to the solid complex. This was in contrast to the usual procedure, where degassing of solvent was accomplished by an argon purge. The degassed solutions of RuTPP(n-$Bu_3P)_2$ did not now effect any decarbonylation of phenylacetaldehyde over several hours. In a further series of experiments, varying pressures of oxygen were admitted to the reaction mixtures after degassing had taken place, Figure V.9. In these cases the reaction proceeded only after O_2 had been admitted; the reactions yielded pseudo-first-order rate constants as usual (Table V.1). It was concluded that trace amounts of O_2 were necessary for stoichiometric decarbonylation. The CH_2Cl_2 solvent used in these experiments had not been routinely degassed since it had been distilled under argon and was considered to be argon-saturated. The aldehyde, distilled in vacuo and stored under argon, was also presumed to be O_2 free. The RuTPP(n-$Bu_3P)_2$ complex itself does not react with O_2 in solution over a period of several days

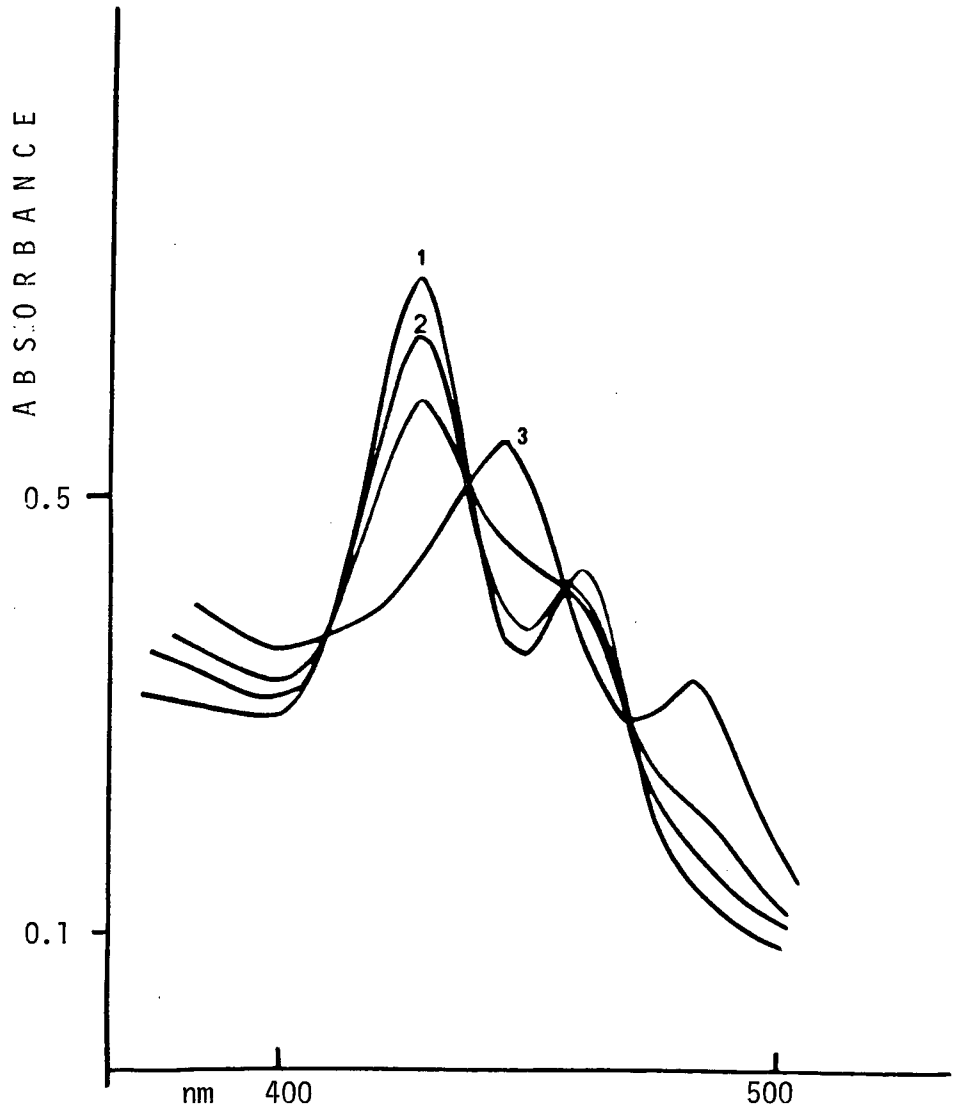

Figure V.9. The Reaction of RuTPP(n-Bu_3P)$_2$ with 3.42×10^{-2}M Phenylacetaldehyde. (1) Initial Spectrum.
(2) 10% Reaction after 30 Min, No Oxygen Admitted.
(3) Final Spectrum, 60 Min after Addition of Oxygen

at ambient temperatures. Visible light does not appear to be a factor since a reaction which was carried out in the dark, except for 30 second intervals to record absorbances, proceeded in the usual manner, i.e. a pseudo-first-order decay of starting material.

An attempted decarbonylation reaction, in which a radical inhibitor (2,6 ditert-butyl-p-cresol) was added to the solvent in ca. 10^{-2}M concentration before dissolution of the solid RuTPP(n-$Bu_3P)_2$, failed to proceed; no change in colour or spectral characteristics was observed after 3 hours, the normal time for these reactions to go to completion.

5.5 Discussion

The oxidation of RuTPP(n-$Bu_3P)_2$ yielded the expected product, Ru(III)TPP(n-$Bu_3P)_2^+$, identified by its visible spectrum. Figure V.10 shows the spectrum obtained for the analogous Ru(III)OEP$(Bu_3P)_2^+$ and Ru(III)TPP$(PPh_3)_2^+$ complexes, the former being produced by electrochemical oxidation and the latter by Br_2 oxidation.[64] The oxidation is reversible since addition of TBAB to solutions of Ru(III)TPP(n-$Bu_3P)_2^+$ regenerates the starting material. An excess of tri-n-butylphosphine also seems to act as a reducing agent.

Oxidation of Ru(porp)(CO)L species is generally thought to occur at the porphyrin ring, rather than at the metal centre, yielding π-cation radical species. Ru(II) π-cation radical species have been well characterized by their u.v.-visible spectra, and also by e.s.r. data. Recent studies in this laboratory have shown that oxidation of RuOEP(CO)L (L = py) gives rise to two different products both π-cation radicals,[64] see Figure V.11. The existence of two possible electronic states for π-cation radicals is well-known, and the formation of one or other of these states seems to depend on the axial ligand, the counter ion present, and the nature of the porphyrin.[65]

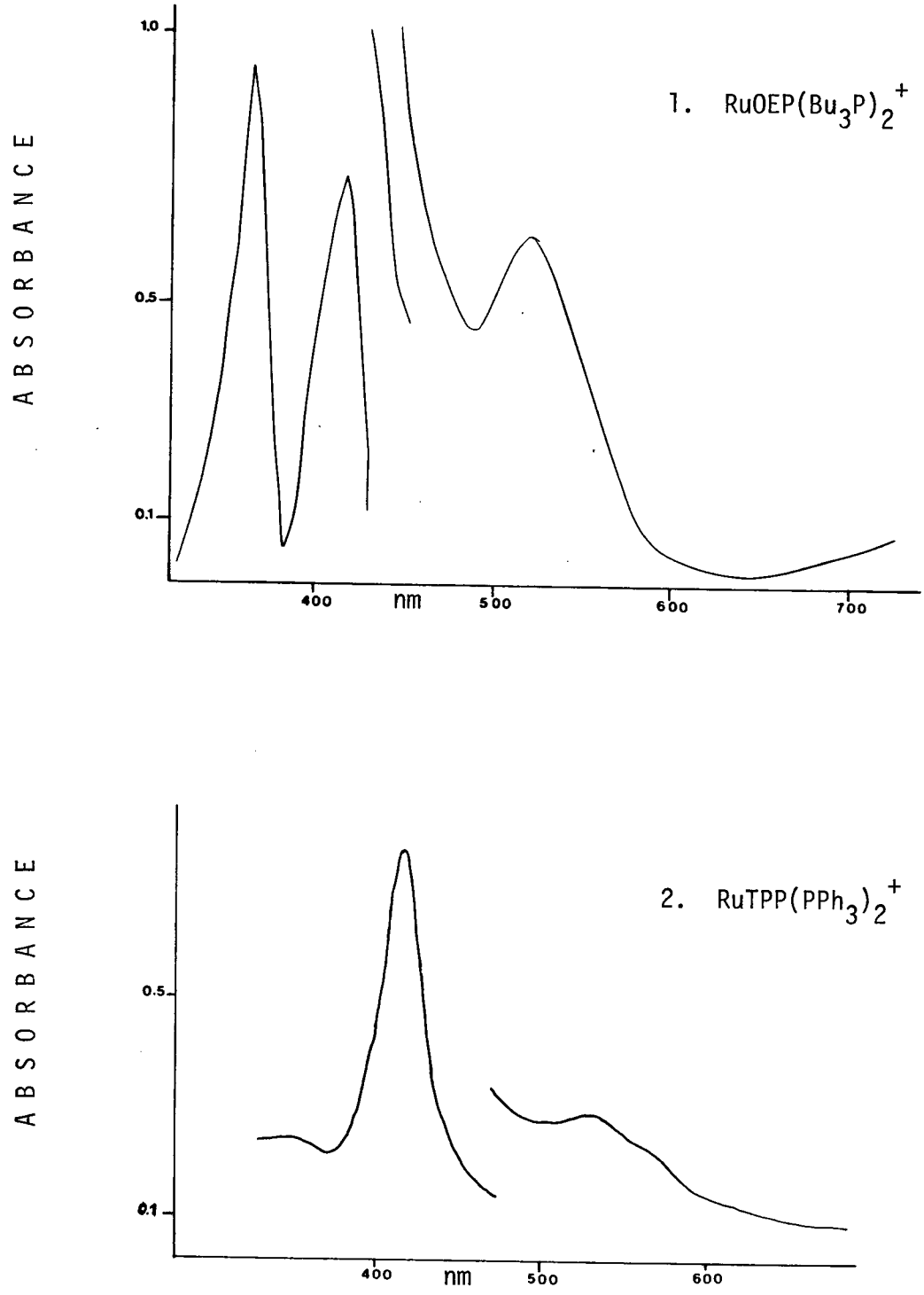

Figure V.10. Spectra of Two Ru(III) Porphyrin Species

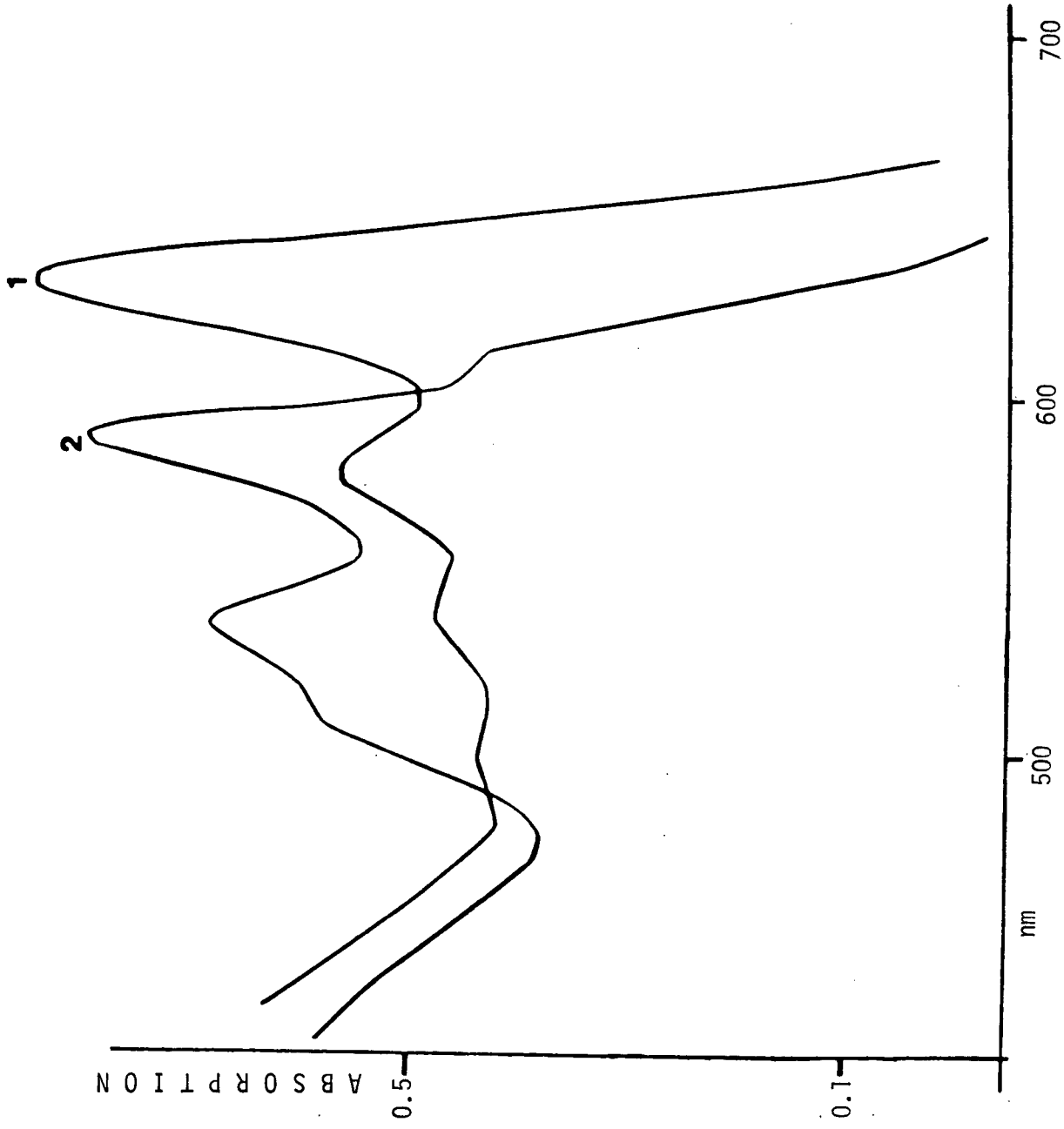

Figure V.II. Spectra of Two π-Cation Radicals Produced by (1) Bromine and (2) Electrochemical Oxidation of RuOEP(CO)(py)

Bromine oxidation of RuTPP(CO)(n-Bu_3P), from the spectral data, does not result in the formation of a π-cation radical but a Ru(III) complex. Electrochemical oxidation does result in the formation of $RuTPP^{+\cdot}(CO)L$, as judged by spectral data and chemical reactivity. The spectrum of this carbonyl oxidation product may be compared with those of various other π-cation radicals, shown in Figure V.12. The general similarities, decreased and broadened Soret bands at ca. 400nm, broad peaks from 500-600nm, and absorption above 600nm, are easily noted. Obviously the change in metal will modify the spectral characteristics as will the solvent. From the spectrum of the reduced species, Figure V.8, it appears that some ligand exchange has occurred, producing mainly RuTPP(CO)S and some RuTPP(n-$Bu_3P)_2$, which suggests that phosphine may have been lost by the π-cation radical allowing acetonitrile, which is in large excess, to coordinate instead. The free phosphine released would then react with the carbonyl complex to give the bis-phosphine complex. The spontaneous regeneration of RuTPP(CO)(S) from solutions of the π-cation radical standing under argon, probably due to trace amounts of reducing agent in the solvent, is also typical of these ruthenium(II) cation radical species, although some cation radicals were found to be quite stable in solution.[65c] As yet no e.s.r. studies have been carried out on this product to confirm the nature of the cation radical.

It was hoped that a study of the redox properties of these two complexes, RuTPP(CO)(n-Bu_3P) and RuTPP(n-$Bu_3P)_2$, would be of aid in explaining the non-catalytic decarbonylation of phenylacetaldehyde, equation V.1. It is probable that some impurity in the aldehyde is responsible for oxidation of either starting material or product thus resulting in the loss of isosbestics after approximately 70% reaction, and generation of a second set of isosbestics seems to support this idea.

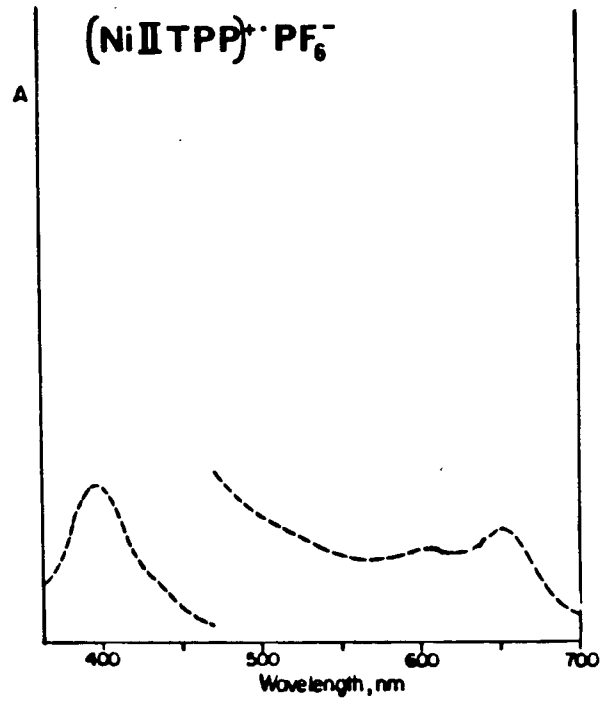

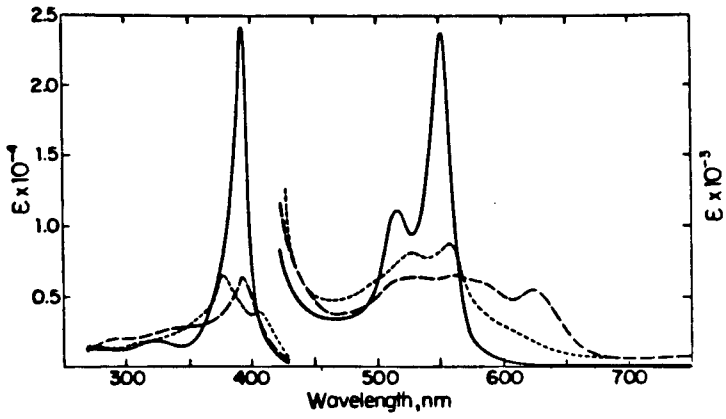

Optical absorption spectra (in CH_2Cl_2) of Co(II)OEP (———); $[Co(III)OEP]^+ClO_4^-$ (— — —); and $[Co(III)OEP]^{2+}\ 2ClO_4^-$ (- - - -).

Figure V.12. Spectra of π-Cation Radicals

Examination of the spectral data indicates that it is oxidation of the metal, giving a ruthenium(III) species, which is occurring, see Figure V.13. The broad absorbance ca. 360nm and general broadening in the

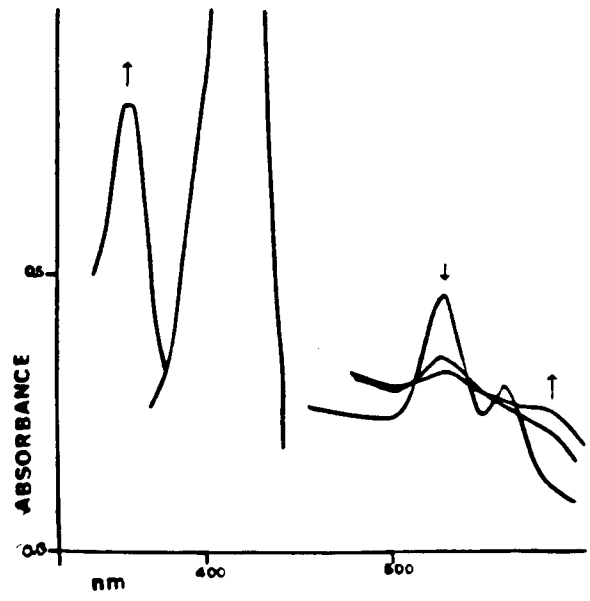

Figure V.13. The Reaction of RuTPP(n-$Bu_3P)_2$ with Phenylacetaldehyde to Give a Ru(III) Species

region 500-600nm is typical of Ru(III) and the spectral changes are more typical of Ru(III)TPP(n-$Bu_3P)_2^+$ than Ru(III)TPP(CO)(n-$Bu_3P)^+$, which has weaker absorbance below 400nm than the bis-phosphine species. This agrees with the observation that RuTPP(n-$Bu_3P)_2$ has a lower oxidation potential (0.5V) than the corresponding carbonyl, since CO tends to stabilize the lower valence state.[44] It would be expected that in a reaction mixture containing both the bis-phosphine and carbonyl complex, the bis-phosphine complex would be preferentially oxidized. Thus it was concluded that the failure of reaction V.1 to go to completion was due, not to the setting

up of an equilibrium, but to the interference of a secondary reaction involving oxidation of the starting material, $RuTPP(n\text{-}Bu_3P)_2$.

Another important feature of this reaction is the influence of O_2 on the progress of the decarbonylation. Since efficiently degassing the solvent effectively inhibits the decarbonylation of phenylacetaldehyde it appears that trace O_2 is necessary for initiation and/or propagation of the reaction. It is not clear from the graph, Figure V.14, if there is any linear dependence of the reaction rate on pO_2. The large variations in k obsd values, Table V.1, may also be explained by this O_2 'dependence', especially as there is a relatively large variation from batch to batch compared with the variations found within each batch. The different batches are sets of data obtained at different times, using different batches of solvent and aldehyde. The complete inhibition of the reaction by a radical inhibitor suggests that O_2 may be initiating the reaction via a free radical process. Organic oxidations frequently require O_2 as a reagent and many of these reactions are free radical processes. One such reaction, the oxidation of methacrolein, is carried out in the presence of a metal catalyst, usually a Co complex.[66] A kinetic study of this reaction indicated a dependence on the first power of the O_2 pressure. This effect of O_2 was ascribed to its role in the abstraction of aldehyde hydrogen by the metal catalyst in the initiation step of the reaction

$$M^{n+} + RCHO \longrightarrow M^{(n-1)+} + R\dot{C}O + H^+$$

since the first step of the reaction was thought to involve coordination of the aldehyde, part of the abstraction of H may have been accelerated by the presence of O_2.

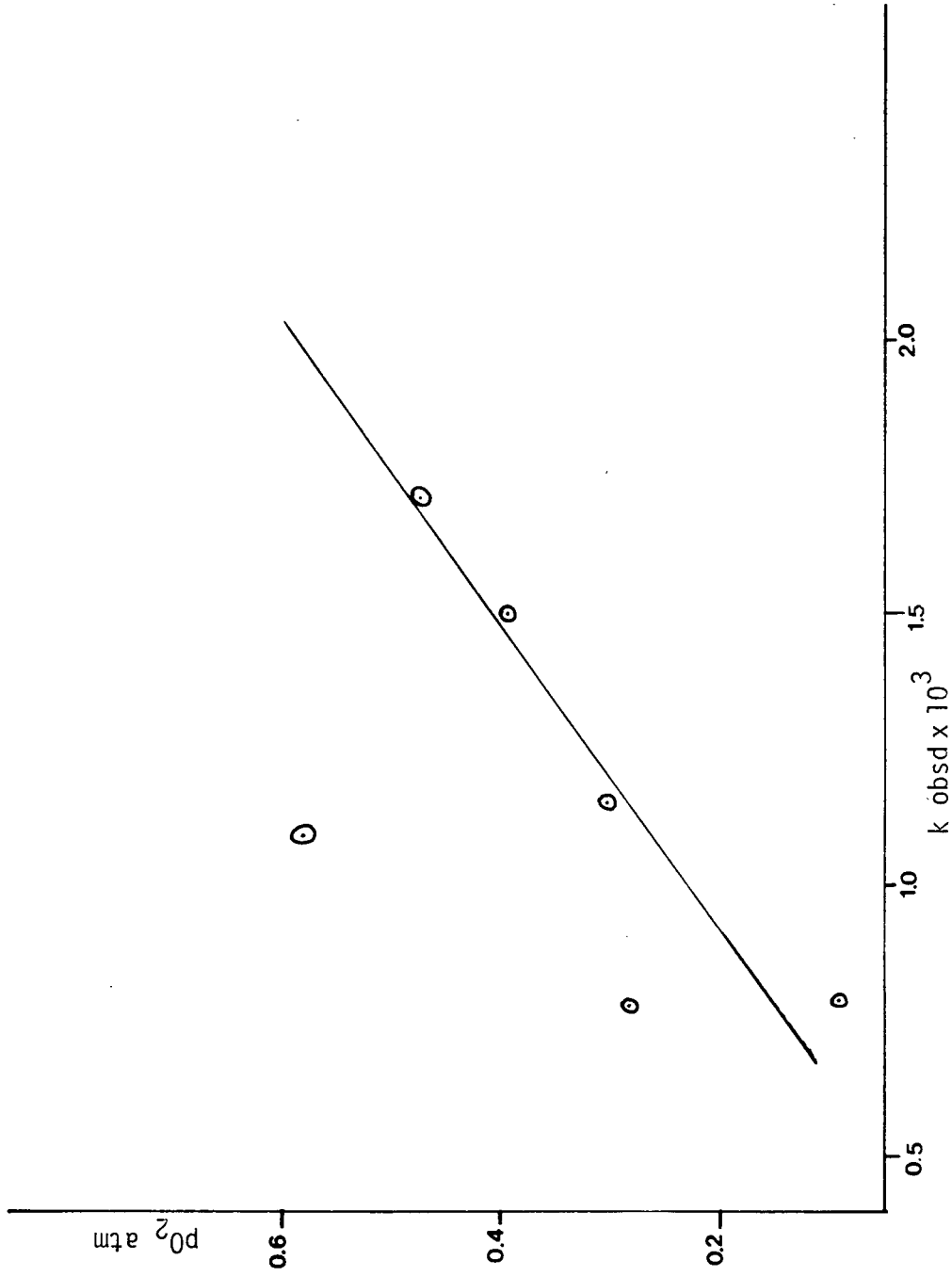

Figure V.14. A Plot of pO_2 Versus k obsd for the Reaction of $RuTPP(n\text{-}Bu_3P)_2$ with Phenylacetaldehyde

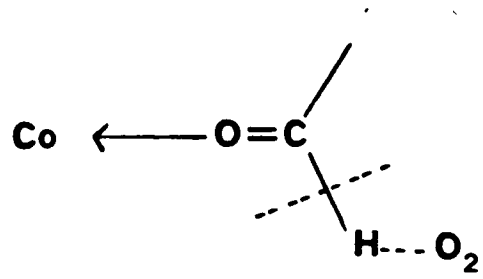

However, this explanation did not fully account for the oxygen dependence of the reaction.[67]

This effect of oxygen, aiding in the abstraction of aldehyde hydrogen, is a possibility for the stoichiometric decarbonylation reaction where the first step may be formation of a Ru(III)H and a radical. However, more data on the effect of oxygen are needed before the details of this reaction are elucidated. The question of whether trace oxygen is a factor in the catalytic decarbonylation reaction, which is thought to proceed via a free radical mechanism, remains although some reactions have been carried out in degassed solvents (freeze-thaw) in attempts to improve reproducibility, no significant effect was observed. However, this does not rule out the possibility of oxygen playing a role since trace oxygen may not have been totally excluded.

CHAPTER 6

CONCLUSIONS

The $RuTPP(n\text{-}Bu_3P)_2$ complex reacted with CO in toluene to give an equilibrium mixture with $RuTPP(CO)(n\text{-}Bu_3P)$. The CO is easily displaced by an excess of tri-n-butylphosphine. Large excesses of tri-n-butylphosphine inhibited the reaction entirely and added excess phosphine is not necessary for pseudo-first-order kinetics. Kinetic and thermodynamic parameters were obtained for this system and the values compared with those found for other $Ru(porp)L_2$ systems and also some porphyrin and Pc systems containing Fe. A structure for the postulated five-coordinate intermediate is proposed, based on a comparison of the k_{-1}/k_2 values. It was concluded that all three $Ru(porp)L_2$ species investigated, and possibly $RuPcL_2$ species, have five-coordinate intermediates whose structures are similar, with the metal atom in the plane of the porphyrin and of low or intermediate spin. A comparison of the k_{-1}/k_2 for two $MTPPL_2$ systems suggests that the nature of the metal influences the structure of the five-coordinate intermediate, the $FeTPPL_2$ intermediate tending to be high spin with the metal more out of the porphyrin plane. Inspection of the K values for the analogous $RuTPP(CO)(n\text{-}Bu_3P)$ and $RuOEP(CO)(n\text{-}Bu_3P)$ complexes implies that the porphyrin has a strong influence on the equilibrium constant. Two possible reasons for this effect were cited: steric hindrance in the TPP sytem causing an increase in the value of k_{-1} and thus increasing K, and the difference in porphyrin basicities, TPP being less basic than OEP.

The $RuTPP(PPh_3)_2$ complex, with added tri-n-butylphosphine in acetonitrile-dichloromethane, was found to be an efficient decarbonylation catalyst for some organic aldehydes. Susbstituted benzaldehydes were decarbonylated more readily than benzaldehyde. The decarbonylation

was inhibited by radical inhibitors. Decarbonylation of cyclohexanecarboxaldehyde resulted in the production of some methylcyclopentane ascribed to the fragmentation of a radical species, $R\dot{C}O$. Other studies, e.g. e.s.r., cyclic voltammetry and i.r. suggested that Ru(III) intermediates were involved as well as free radicals. The existence of a solvated species in the catalyst solutions was indicated by spectral evidence. The dissociation of $RuTPP(PPh_3)_2$ and $RuTPP(CO)(PPh_3)$ in dilute solution indicated that some solvated species, such as RuTPP(CO)(S), is likely to play an important role in the catalytic decarbonylation.

The stoichiometric reaction between $RuTPP(n\text{-}Bu_3P)_2$ and phenylacetaldehyde did not go to completion. However, a possible equilibrium involving toluene was ruled out and a secondary reaction, probably oxidation of $RuTPP(n\text{-}Bu_3P)_2$, is considered to be the reason for the observed 'equilibrium.' Pseudo-first-order kinetics were observed for this reaction in the absence of added phosphine. In the presence of stoichiometric amounts of tri-n-butylphosphine the reaction failed to proceed. The pseudo-first-order rate constants calculated were irreproducible and scattered, implying that radical formation might be implicated in a rate determining step. Trace oxygen was necessary for the initiation and/or propagation of the stoichiometric decarbonylation.

Suggestions for Further Study

As regards the study of the carbonylation reaction it would be interesting to obtain more data on RuTPP and other Ru porphyrin systems in order to generate a more complete picture.

The main problem in obtaining more concrete evidence of intermediates, etc., in the catalytic reaction is the insolubility of the TPP complexes in acetonitrile solution. The possibility of detecting and

isolating intermediates would increase if the catalyst solutions were more concentrated; collection and identification of products would also be facilitated. One way to increase the solubility of the porphyrin is to attach hydrocarbon 'tails', which could be accomplished without serious difficulty as TPP is the easiest and cheapest synthetic porphyrin to make. There is, however, the possibility that any such modification to the porphyrin might adversely affect its catalytic activity.

As free radicals seem to be implicated in the catalysis, some deuteration studies might prove useful. A possible experiment is the decarbonylation of a mixed aldehyde and deutero-aldehyde system. This type of experiment would indicate whether or not a bimolecular pathway was involved. Deuteration at the aldehyde hydrogen of cyclohexanecarboxaldehyde, for instance, may provide some information about the nature of the proposed radical intermediate. Kinetic isotope studies would give some indications about the rate determining step although rate constants were found to be nonreproducible. All of these experiments would also profit from increased catalyst concentration yielding larger quantities of product to investigate.

One of the major flaws in this catalytic system is the lack of long term stability, which combined with poor solubility, prevents the accumulation of decarbonylated products. It is not clear how the catalyst is destroyed. Certainly the spectra indicate that some metal oxidation occurs, probably again due to trace impurities in the aldehydes; free radicals are also likely candidates for attack on the porphyrin ring. Development of more sophisticated techniques for aldehyde purification may be worthwhile, however, if free radicals are responsible then it appears likely that this lack of stability is an unavoidable feature of the experiment.

REFERENCES

1. J. Tsuji and K. Ohno, Synthesis, 157 (1969).
2. C.W. Bird, 'Transition Metal Intermediates in Organic Chemistry', Logos Press, London, 1967.
3. A. Kozikowski and H. Wetter, Synthesis, 561 (1976).
4. M.C. Baird, C.J. Nyman and G.W. Wilkinson, J. Chem. Soc. (A), 348 (1969).
5. K. Ohno and J. Tsuji, J. Am. Chem. Soc., 90, 99 (1968).
6. R.H. Prince and K.A. Raspin, J. Chem. Soc. (A), 612 (1969).
7. J.K. Stille, M.T. Regan, R.W. Fries, F. Huang and T. Mc-Carly, Adv. Chem. Series, 132, 181 (1974).
8. J. Blum, E. Oppenheimer and E.D. Bergman, J. Am. Chem. Soc., 89, 2338 (1967).
9. R.R. Schrock and J.A. Osborne, J. Am. Chem. Soc., 93, 2397 (1971).
10. J.K. Stille and M.T. Regan, J. Am. Chem. Soc., 96, 1508 (1974).
11. M.C. Baird, J.T. Mague, J.A. Osborne and G.W. Wilkinson, J. Chem. Soc. (A), 1347 (1967).
12. D.L. Egglestone, M.C. Baird, C.J.L. Lock and G. Turner, J.C.S. Dalton, 1576 (1977).
13. K.S.Y. Lau, Y. Becker, F. Huang, N. Baenziger and J.K. Stille, J. Am. Chem. Soc., 99, 5664 (1977).
14. J. Blum, S. Kraus and Y. Pickholtz, J. Organomet. Chem., 33, 227 (1971).
15. C.A. Tolman, P.Z. Meaken, D.L. Lindner and J.P. Jessen, J. Am. Chem. Soc., 96, 2762 (1974).
16. J. Halpern and C.S. Wong, J.C.S. Chem. Comm., 629 (1973).

17. J.A. Osborne,F.H. Jardine, J.F. Young and G. Wilkinson, J. Chem. Soc. (A), 1711 (1966).

18. G.L. Geoffroy, D.A. Denton, M.E. Keeney and R.R. Bucks, Inorg. Chem., 15, 2382 (1976).

19. W. Stroiheimer and P. Pfohler, J. Organomet. Chem., 108, 393 (1976).

20. J.W. Suggs, J. Am. Chem. Soc., 100, 640 (1978).

21. T.B. Rauchfuss, Fundamental Research in Homogeneous Catalysis, Vol. 3, 1979, p. 1021.

22. F.A. Cotton and G. Wilkinson, 'Advanced Inorganic Chemistry', Third Edition, Interscience, New York, 1972, p. 1000.

23. J. Tsuji and K. Ohno, J. Am. Chem. Soc., 90, 94 (1968).

24. H.E. Eschinazi and H. Pines, J. Org. Chem., 21, 1369 (1959).

25. D.H. Doughty and L.H. Pignolet, J. Am. Chem. Soc., 100, 7083 (1978).

26. D.H. Doughty, F.M. Mcguiggan, M. Wang and L.H. Pignolet, Fundamental Research in Homogeneous Catalysis, Vol. 3, 1979, p. 909.

27. B.D. Berezin, 'Coordination Compounds of Porphyrins and Phthalocyanines', Wiley, New York, 1981.

28. J.P. Collman, M. Marrocco, P. Denisovich, C. Koval and F.C. Anson, J. Am. Chem. Soc., 100, 117 (1980).

29. J.Y. Becker, D. Dolphin, J.B. Paine III and S.F.B. Pickett, unpublished results.

30. G. Domazetis, B. Tarpey, D. Dolphin and B.R. James, J.C.S. Chem. Comm., 939 (1980); A.C.S. Symposium Series, 152, 243 (1981).

31.(a) B.C. Chow and I.A. Cohen, Bioinorganic Chem., 1, 57 (1971).

(b)M. Tsutsui, D. Ostfeld and L.M. Hoffman, J. Am. Chem. Soc., 93, 1820 (1971).

(c) S.S. Eaton, G.R. Eaton and R.H. Holm, J. Organomet. Chem., 39, 179 (1972).

(d) D. Cullen, E. Meyer Jr., S. Shrivastava and M. Tsutsui, J.C.S. Chem. Comm., 584 (1972).

32. J.J. Bonnet, S.S. Eaton, G.R. Eaton, R.H. Holm and J. Ibers, J. Am. Chem. Soc., 95, 2141 (1973).

33. D. Dolphin, A.W. Addison, M. Cairns, R.K. DiNello, N. Farrell, B.R. James, D.R. Paulson and C. Welborn, Int. J. Quantum Chem., Vol. XVI, 311 (1979).

34. C.K. Chang, D. Dowell and T.G. Traylor, Croat. Chem. Acta, 49, 295 (1973).

35. N. Farrell, D.H. Dolphin and B.R. James, J. Am. Chem. Soc., 100, 324 (1978).

36. D.V. Stynes, H.C. Stynes, B.R. James and J.A. Ibers, J. Am. Chem. Soc., 95, 4087 (1973).

37. D.V. Stynes and B.R. James, J.C.S. Chem. Comm., 325 (1973).

38. C.J. Weschler, D.L. Anderson and F. Basolo, J. Am. Chem. Soc., 97, 6707 (1975). J.C.S. Chem. Comm., 757 (1974).

39. B.R. James, A.W. Addison, M. Cairns, D. Dolphin, N.P. Farrell, D.R. Paulson and S.G. Walker, Fundamental Research in Homogeneous Catalysis, Vol. 3, 1979, p. 751.

40. D.R. Paulson, A.W. Addison, D. Dolphin and B.R. James, J. Biol. Chem., 254, 7002 (1979).

41. S.G. Walker, M.Sc. Thesis, University of British Columbia, 1980.

42. F.R. Hopf, T.P. O'Brien, W.R. Scheidt and D.G. Whitten, J. Am. Chem. Soc., 97, 277 (1975).

43. T. Boschi, G. Bontempelli and G.A. Mazzochin, Inorg. Chim. Acta, 37, 155 (1979).

44. G. Domazetis, private communication.

45. 'The Manipulation of Air Sensitive Compounds', D.F. Shriver, McGraw-Hill, New York, N.Y., 1969.

46. A. Seidell, 'Solubilities of Inorganic and Metal Organic Compounds', Vol. I, Third Edition, D. Van Nostrand Co., New York, N.Y. 1970.

47. I. Amdur and G. Hammes, 'Chemical Kinetics, Principles and Selected Topics', McGraw-Hill, New York, N.Y., 1962, p. 12,

48. J.E. Falk, 'Porphyrins and Metalloporphyrins', Elsevier Publishing Co., New York, N.Y., 1964.

49. D. Kent, B.Sc. Thesis, University of British Columbia, 1973.

50. W.A. Graham, Inorg. Chem., 7, 315 (1968).

51. B.R. James and D.V. Stynes, J. Am. Chem. Soc., 96, 2733 (1974).

52. A. Antipas, J.W. Buchler, M. Gouterman and P.D. Smith, J. Am. Chem. Soc., 102, 198 (1980).

53. M.M. Doeff and D.A. Sweigart, Inorg. Chem., 20, 1683 (1981).

54. J. Martinson, M. Miller, D. Trojan and D.A. Sweigart, Inorg. Chem., 19, 2162 (1980).

55. Structural studies have indicated that porphyrins may be somewhat less rigid than phthalocyanine, see 'The Porphyrins', Vol. II B, ed. D. Dolphin, Academic Press, New York, N.Y., 1978.

56. J.J. Bonnet, S.S. Eaton, G.R. Eaton, R.H. Holm and J.A. Ibers, J. Am. Chem. Soc., 95, 2141 (1973).

57. G. Domazetis, private communication.

58. D. Dolphin, B.R. James, A.J. Murray and J.R. Thornback, Can. J. Chem., 58, 1125 (1980).

59. J.W. Wilt in 'Free Radicals', Vol. I, ed. J.K. Kochi, Wiley, New York, N.Y., 1973.

60. H.M. Walborsky and L.E. Allen, J. Am. Chem. Soc., 93, 5465 (1971).

61. E.A. Guggenheim, Phil. Mag., 2, 538 (1962).

62. A. Brandstrom, U. Junggren and B. Lamm, Tet. Lett., 3173 (1972).

63. G.M. Brown, F.R. Hopf, J.A. Fergussen, T.J. Meyer and D.G. Whitten, J. Am. Chem. Soc., 95, 5385 (1975).

64. M. Barley, private communication.

65.(a)C. Weiss, H. Kobayashi and M. Gouterman, J. Mol. Spectrosc., 16, 415 (1965).

(b)J. Fajer, D.C. Borg, A. Forman, R.H. Felton, L. Vegh and D. Dolphin, J. Am. Chem. Soc., 92, 3451 (1970).

(c)D. Dolphin and R.H. Felton, Acc. Chem. Res., 7, 26 (1974).

66. W.F. Brill and F.J. Lister, J. Org. Chem., 26, 565 (1961).

67. 'The Oxidation of Organic Compounds', A.C.S. Advances in Chemistry Series, 75, ed. R.F. Gould, 1968, p. 126.